# MONTHLY WEATHER REVIEW

VOLUME 78 NUMBER 7

## JULY 1950

CONTENTS



U. S. DEPARTMENT OF COMMERCE · WEATHER BUREAU

## CORRECTION

MONTHLY WEATHER REVIEW, June 1950, vol. 78, No. 6: In the article by Carson (pp. 91–101), the legends to figures 6, 8, 13, 14, and 16 should be changed so that the heavy solid line on the left is described as dew-point temperature, not potential pseudo-wet-bulb temperature.

DEPARTMENT OF COMMERCE
CHARLES SAWYER, Secretary

WEATHER BUREAU
F. W. REICHELDERFER, Chief

# MONTHLY WEATHER REVIEW

Editor, JAMES E. CASKEY, Jr.

Volume 78
Number 7

JULY 1950

Closed Sept. 5, 1950
Issued October 15, 1950

## A NUMERICAL METHOD FOR FORECASTING RAINFALL IN THE LOS ANGELES AREA

J. C. THOMPSON [1]

Weather Bureau Airport Station, Los Angeles, California
[Manuscript received June 16, 1950]

### ABSTRACT

The application of modern statistical methods to the forecasting of rainfall in Los Angeles is discussed. Forecasts are made by graphical integration of a number of objective meteorological variables and the results presented in terms of the probability of rainfall occurring in each of several amount categories. The accuracy of this technique is discussed and compared with that obtained by current conventional forecasting methods, while the precision of the probability estimates is compared with a subjective evaluation of the probability distribution. Both comparisons show a slight, but statistically nonsignificant bias in favor of the numerical method.

The probability forecasts are shown to provide additional information regarding the reliability of each prediction which, by applying the principle of calculated risk, may be used to minimize the cost of carrying on any repetitive operation. An example of the use of this type of forecast is given, showing the saving which would result in a typical industrial operation in Los Angeles during the winter season of 1949–50.

### CONTENTS



### INTRODUCTION

As part of an extensive research program instituted by the U. S. Weather Bureau for the general purpose of improving the accuracy and usefulness of short-range weather forecasts, a study of the application of statistical methods to the forecasting of winter rainfall in Los Angeles was begun during the summer of 1945. Following publication of the preliminary results a year later [1], a project to continue the investigation was established as a cooperative effort of the Weather Bureau and the University of California at Los Angeles. This investigation was continued for a two year period, covering a number of different methods of analysis, types of presentation and forecast periods [2, 3].

The study indicated that, for many industrial, agricultural, and military operations, some advantages are to be obtained from the use of numerical methods in weather forecasting. In general, these advantages ensue from the increased efficiency provided in preparation of the forecast, as well as from the fact that additional information may be made available by the inclusion of a reliability index for each prediction. Due to space restrictions, the following discussion does not cover the entire investigation, but only describes one of the most promising of the methods, shows how it was derived, indicates the nature and accuracy of the forecast it provides and, finally, gives an example of how the forecast may be used to best advantage.

[1] Now in Short Range Forecast Development Section, U. S. Weather Bureau, Washington, D. C.

903939—50——1

## FORECAST PERIOD

The forecast of greatest public distribution and usefulness for the Los Angeles area is issued a short time before the beginning of the normal business day. It describes the weather to be expected during the time beginning at 1030 PST of the current day through 1630 PST of the following day, a period which is denoted in the forecast by the terms "this afternoon, tonight, and tomorrow." In view of the importance of this particular forecast the greater part of the research effort was directed at the development of an objective rainfall forecasting method which would cover this period. Data upon which the forecasts were based were limited to those available by the 0430 PST map time, and the results verified by the rainfall amounts which were observed at the Los Angeles Weather Bureau City Office during the period outlined above. The forecasting method covers the normal winter rainy season, from October 1 through March 31.

## METHOD OF DEVELOPMENT

The forecasting method was developed by use of a graphical integration technique suggested by Brier [4]. Briefly, this process involves the selection of a number of independent (or as nearly independent as possible) meteorological variables which are believed to be related to the weather element to be forecast during some later period. The general procedure is then to work with the variables in pairs, each set of two variables being plotted on a scatter diagram with the independent variables as coordinates and the values of the dependent variate indicated beside each plotted point. In the case of a discrete two-valued variate, the independent variables are combined into a single derived variable by fitting a probability surface to the data, with the values of the probability isopleths used to express the functional relationship between the coordinate variables and the plotted variate. Where the element to be forecast is continuous, the variables are

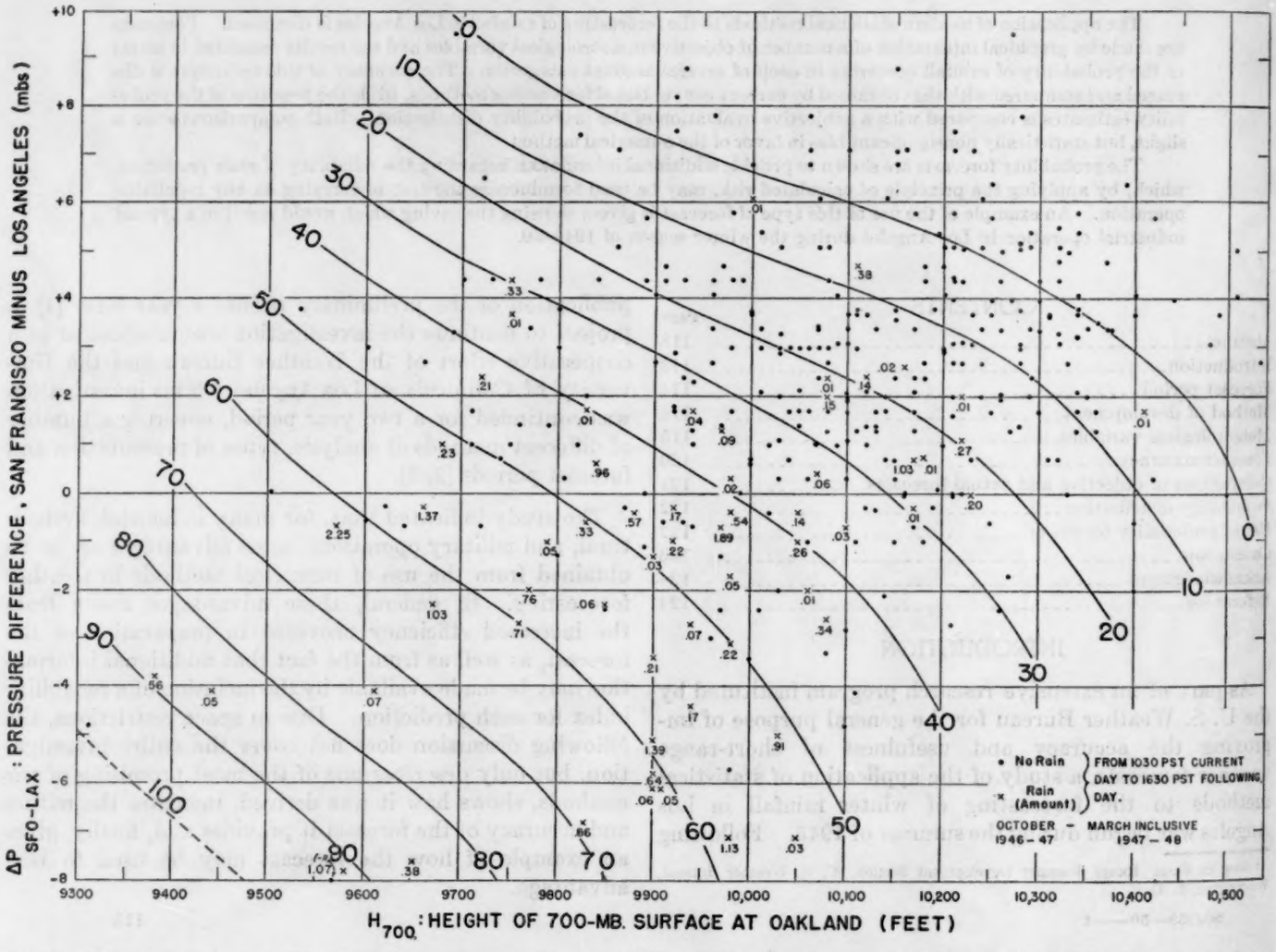


FIGURE 1.—Scatter diagram showing rainfall at Los Angeles as a function of $\Delta P_{SFO-LAX}$ and $H_{700}$. Solid curves are isograms of rainfall amount, adjusted to a scale of 0 to 100. These curves define a single variable $X_1$, which is plotted as the abscissa in figure 4.

combined into a single derived variable by constructing isograms which express the values of the plotted variate.

The derived variables resulting from each pair of original variables are again combined in pairs and the process repeated until finally only one remains. This final derived variable is thus a function of all of the original variables and may accordingly be used to give some information about the weather element it is desired to forecast. A more complete description of the process is thought to be unnecessary here, since a fairly detailed discussion is available in Brier's original paper as well as in several recent forecasting studies by other investigators [5, 6, 7].

The graphical technique has the disadvantage of a certain amount of subjectivity in the original combination of variables, but this is largely outweighed by its relative simplicity as well as the fact that it eliminates the necessity for having prior knowledge of, or making assumptions regarding, the functional relationship between the independent variables and dependent variate, a requirement common to all mathematical regression methods. There is no lack of objectivity in the use of the charts obtained from the graphical analysis.

## METEOROLOGICAL VARIABLES

A large number of meteorological variables which were believed to be of significance in forecasting rainfall were tested, both singly and in various combinations. Here, use was made of the general approach to the problem of quantitative rainfall forecasting outlined by Showalter [8], as well as a particular application to major storms in the Los Angeles Basin presented in a report issued by the Hydrometeorological Section of the U. S. Weather Bureau [9]. Of the relationships tested, the following six variables produced the greatest skill and were incorporated in the final forecasting method:

| | |
|---|---|
| $H_{700}$ | Height of the 700-mb. surface at Oakland, vs |
| $\Delta P_{SFO-LAX}$ | Sea level pressure difference, San Francisco minus Los Angeles. |
| $P_{SFO}$ | Sea level pressure at San Francisco, vs |
| $\Delta P_{LAX-PHX}$ | Sea level pressure difference, Los Angeles minus Phoenix. |
| $D_{SDB}$ | Wind direction at Sandberg, vs |
| $T_{700}$ | Temperature at 700 mb. at Santa Maria. |

Although it is impractical to provide a complete discussion of the reasoning involved in testing of all variables investigated, a brief summary of the causal relationships which suggested the combination of the final six may be of interest.

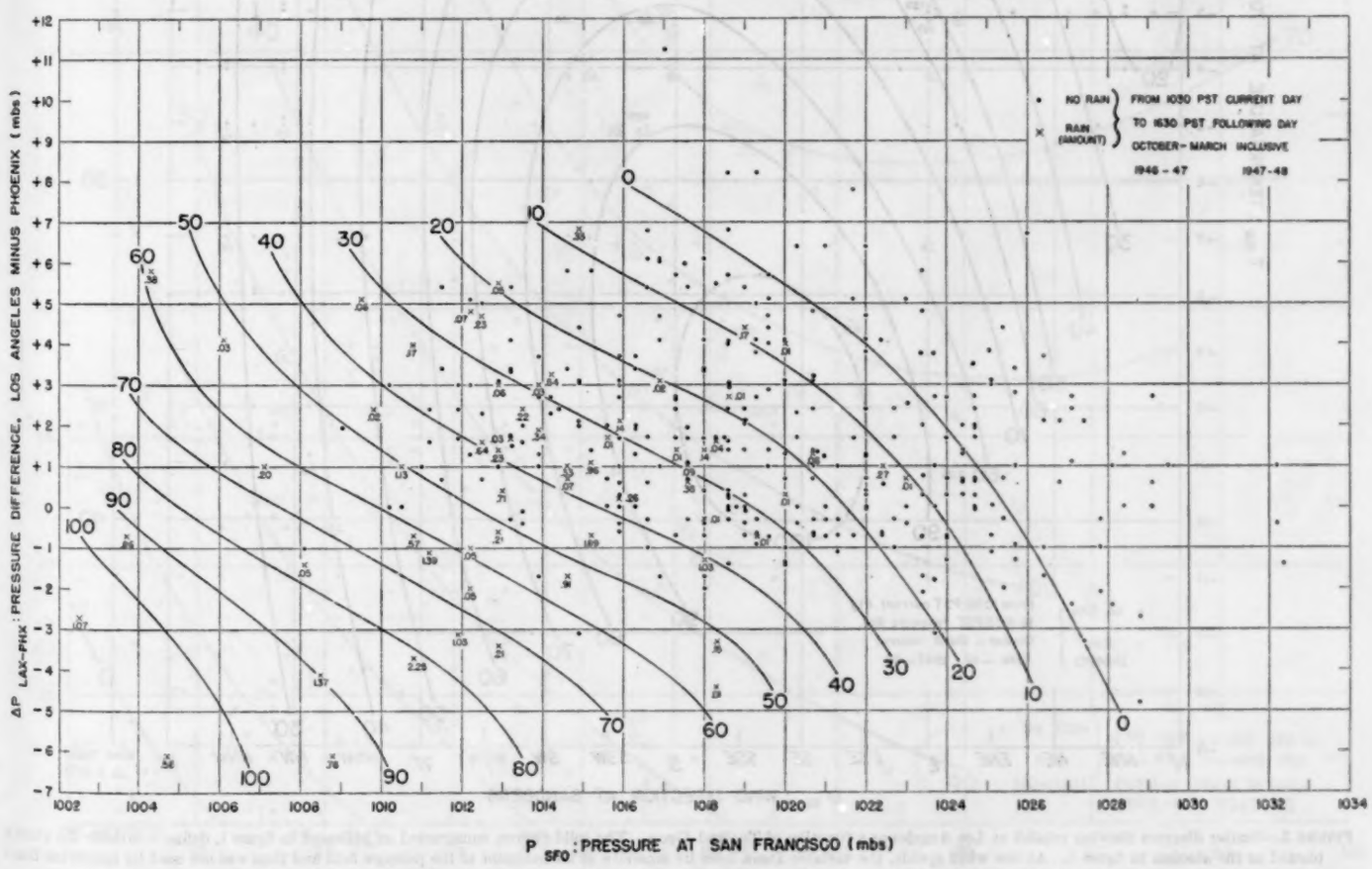


FIGURE 2.—Scatter diagram showing rainfall at Los Angeles as a function of $\Delta P_{LAX-PHX}$ and $P_{SFO}$. The solid curves, constructed as indicated in figure 1, define a variable $X_3$, which is plotted as the ordinate in figure 4.

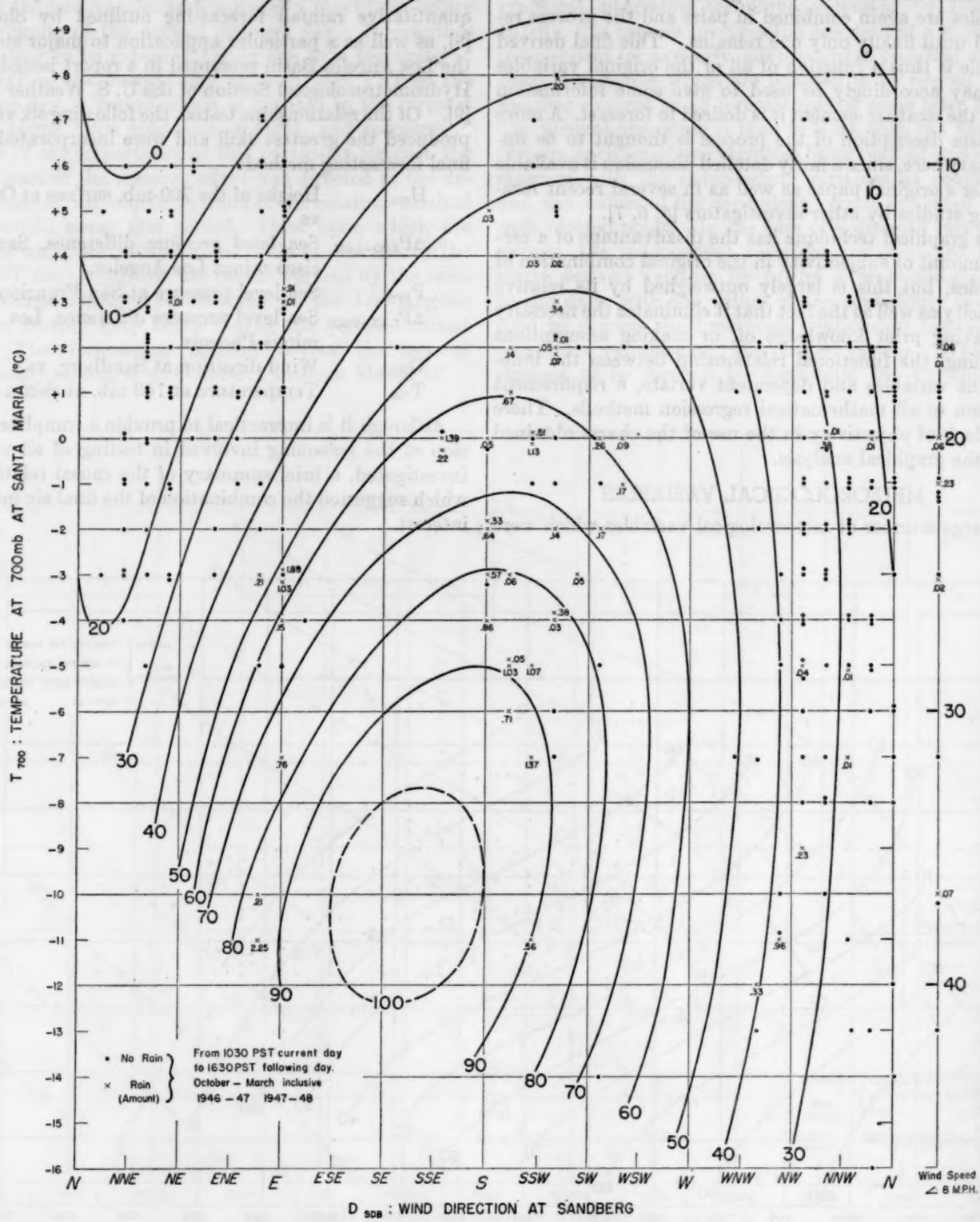


FIGURE 3.—Scatter diagram showing rainfall at Los Angeles as a function of $T_{700}$ and $D_{SDB}$. The solid curves, constructed as indicated in figure 1, define a variable $X_2$, which is plotted as the abscissa in figure 5. At low wind speeds, the variable $D_{SDB}$ loses its sensivity as an indicator of the pressure field and thus was not used for speeds less than 8 m. p. h. These cases were plotted against $T_{700}$ along the vertical axis to the right of the scatter diagram and analyzed separately to determine $X_2$.

It had previously been found that, for storms approaching from any westerly direction, the height of the 700-mb. surface at Oakland is quite well correlated with the distance of the nearest low center [2]. For storms of this type, the sea level pressure difference between Los Angeles and San Francisco, when combined with the distance of the low center, provides a rough measure of the strength of the wind flow across the area and indicates to some extent the isobaric curvature, and hence horizontal convergence, associated with the disturbance. For storms approaching from the east, the above reasoning does not apply, but these are few in number and as a rule only small amounts of rain are associated with them.

When storms move inland a surface trough usually develops over the interior. Thus the sea level pressure difference, Los Angeles minus Phoenix, which is usually

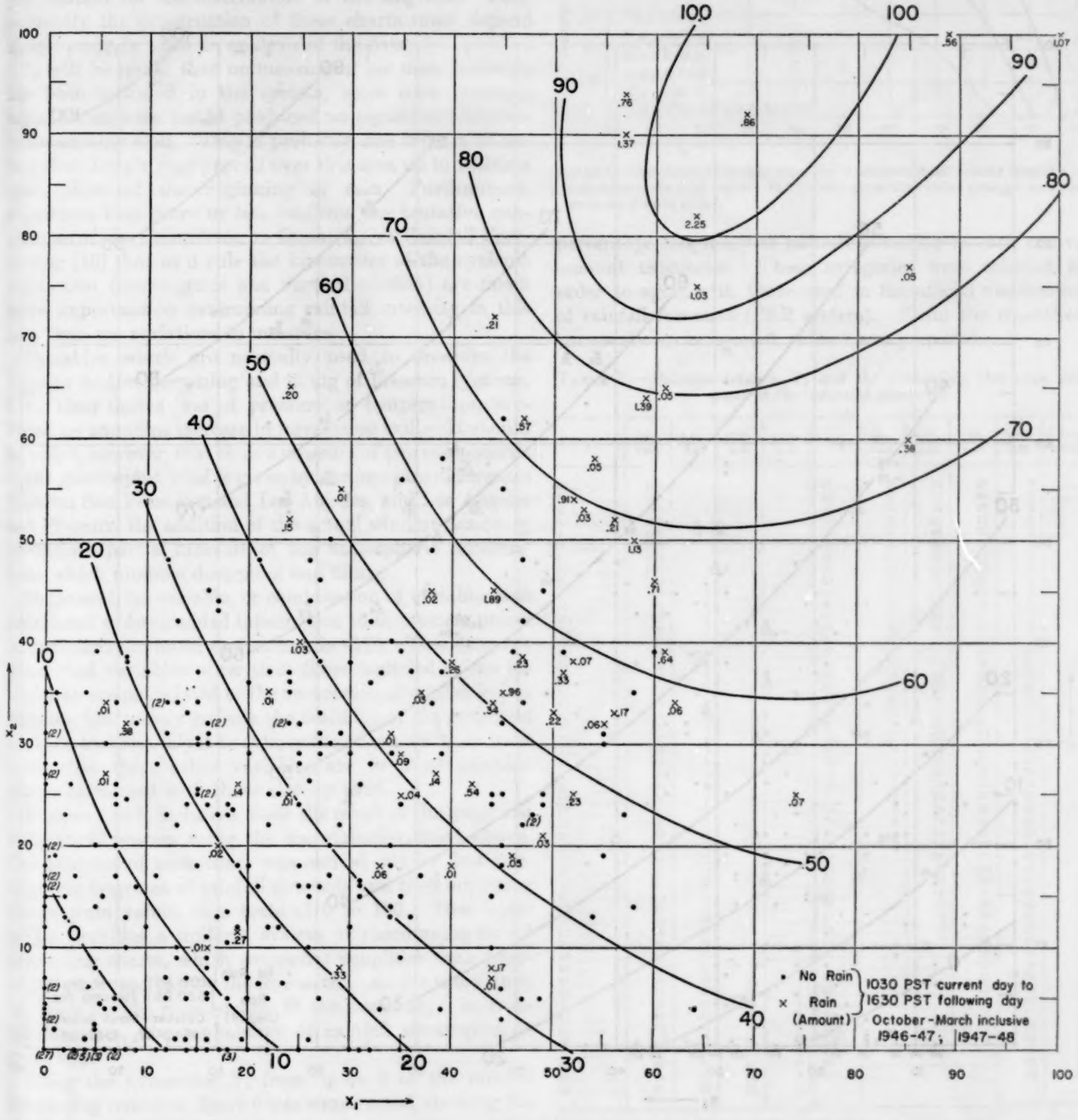


FIGURE 4.—Scatter diagram showing rainfall at Los Angeles as a function of $X_1$ (from fig. 1) and $X_2$ (from fig. 2). The solid curves, constructed as indicated in figure 1, define a variable $Y_1$ which is plotted as the ordinate in figure 5. The number in parentheses under a dot indicates the number of dots falling at that given point.

negative when a storm is situated off the coast, tends to become positive following, or just preceding, the end of the rain. This variable also helps to evaluate the rainfall resulting from easterly storms, which were not considered in the previous combination of variables. When combined with the sea level pressure at San Francisco, negative values of the pressure difference, Los Angeles minus Phoenix, and low values of the pressure at San Francisco are indicative of heavy rain.

The temperature at 700 mb. at Santa Maria provides a crude measure of the air mass stability, while the wind direction at Sandberg has long been used by experienced forecasters in this region as a rainfall forecasting aid to indicate the approach of a storm from the Pacific (southerly winds) or the final passage of a cold front (northerly winds). Winds at that point are apparently much more sensitive to changes in the pressure field than are those in the free air.

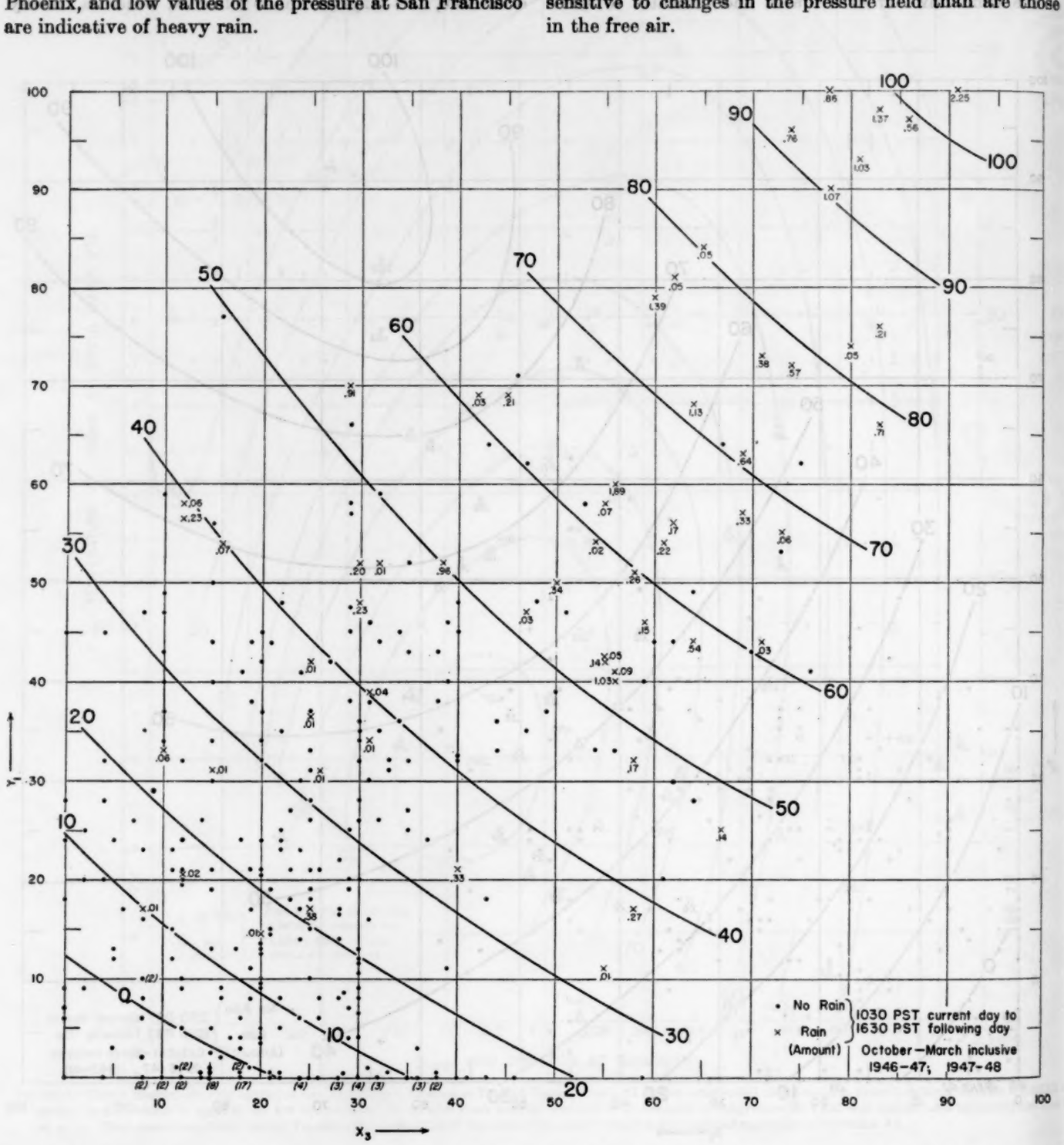


FIGURE 5.—Scatter diagram showing rainfall at Los Angeles as a function of $X_3$ (from fig. 3) and $Y_1$ (from fig. 4). The solid curves, constructed as indicated in figure 1, define a variable $Y_3$, which is plotted as the abscissa in figure 6. The number in parentheses under a dot indicates the number of dots falling at that given point.

While the meteorological relationships brought out by the primary graphical combination of each pair of variables (figs. 1, 2, and 3) may thus be discussed from a physical standpoint, and thereby the reasonableness of the isograms checked, very little can be said about the secondary combinations (figs. 4 and 5). Here the complexity of the joint relationships, as well as the probable effect of other variables not considered in the integration, defeats any attempt to supply a theoretical or physical justification for the distribution of the isograms. Consequently the construction of these charts must depend almost entirely upon an analysis of the data.

It will be noted that no measure of air mass moisture has been included in the system, since such moisture variables as were tested produced no significant increase in forecasting skill. This is probably due in part to the fact that dry air may prevail over this area up to within a short time of the beginning of rain. Furthermore, experience here more or less confirms the tentative conclusions of the Committee on Quantitative Rainfall Forecasting [10] that as a rule the kinematics of the cyclonic circulation (convergence and vertical motion) are much more important in determining rainfall intensity in this area than are variations in moisture.

Variables which are normally used to measure the velocity and/or deepening and filling of pressure systems, i. e., time derivatives of pressure or temperature, produced no apparent increase in forecasting skill. It should be noted, however, that since a measure of two components of the geostrophic wind is given by the pressure differences between San Francisco and Los Angeles, and Los Angeles and Phoenix, the addition of the actual wind at Sandberg provides a partial measure of the atmospheric accelerations which produce deepening and filling.

In general, no variable, or combination of variables was considered to have added information to the system unless its inclusion produced an increase in skill. This does not mean that variables other than those included in the integration are not related to the occurrence of rainfall in Los Angeles, but merely reflects the inability of the graphical analysis and/or analyst to supply the relationship, or indicates that these other variables are to a considerable degree correlated with those already used.

Figures 1 to 5, inclusive, show the result of the graphical integration process using the six variables listed above. The analysis of each chart was carried out by first constructing isograms of rainfall amounts and then adjusting the isogram values to a scale of 0 to 100. This latter device provides a uniform system of coordinates on all succeeding charts, which somewhat simplifies their preparation and final use by the forecaster. At the same time, the basis for the construction of the isograms, i. e., rainfall amounts, not probability of rainfall occurrence, is preserved.

Using the parameter $Y_2$ from figure 5 as the rainfall forecasting criterion, figure 6 was constructed, showing the

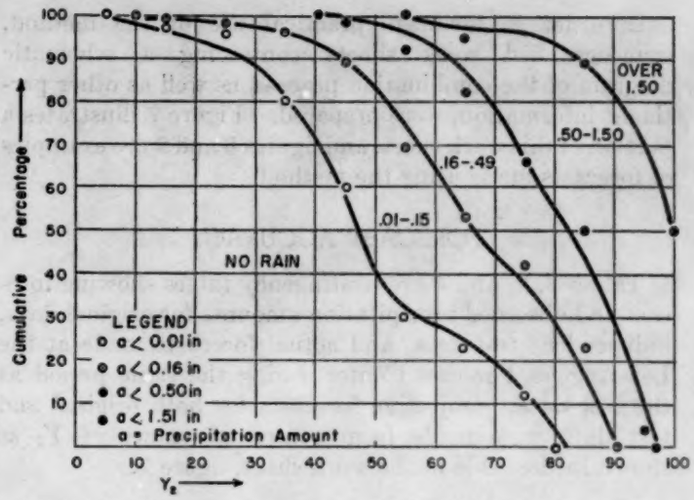


FIGURE 6.—Cumulative percentage frequency of selected rainfall amount categories as a function of the final variable $Y_2$. Rainfall probability values obtained from this graph are given in table 1.

percentage frequency of rainfall occurring in each of five amount categories. These categories were selected in order to agree with those used in the official verification of rainfall forecasts (PFR system). From the smoothed curves shown in figure 6, table 1 was prepared.

TABLE 1.—*Relation between $Y_2$ and the probability that rain will occur in the indicated categories*

| $Y_2$ | No rain | 0.01-0.15 | 0.16-0.49 | 0.50-1.50 | $Y_2$ | No rain | 0.01-0.15 | 0.16-0.49 | 0.50-1.50 | 1.51 or more |
|---|---|---|---|---|---|---|---|---|---|---|
| 0 | 100 | | | | 51 | 38 | 44 | 15 | 3 | |
| 1 | 100 | | | | 52 | 37 | 43 | 16 | 4 | |
| 2 | 100 | | | | 53 | 35 | 44 | 17 | 4 | |
| 3 | 100 | | | | 54 | 34 | 43 | 18 | 5 | |
| 4 | 100 | | | | 55 | 32 | 43 | 20 | 5 | |
| 5 | 100 | | | | 56 | 32 | 42 | 20 | 5 | 1 |
| 6 | 100 | | | | 57 | 31 | 41 | 22 | 5 | 1 |
| 7 | 100 | | | | 58 | 30 | 40 | 23 | 6 | 1 |
| 8 | 99 | 1 | | | 59 | 29 | 38 | 25 | 6 | 2 |
| 9 | 99 | 1 | | | 60 | 28 | 36 | 28 | 6 | 2 |
| 10 | 98 | 2 | | | 61 | 28 | 34 | 29 | 7 | 2 |
| 11 | 98 | 2 | | | 62 | 27 | 32 | 31 | 7 | 3 |
| 12 | 98 | 2 | | | 63 | 26 | 31 | 33 | 7 | 3 |
| 13 | 97 | 3 | | | 64 | 25 | 30 | 33 | 9 | 3 |
| 14 | 97 | 3 | | | 65 | 25 | 27 | 35 | 10 | 3 |
| 15 | 96 | 4 | | | 66 | 24 | 26 | 36 | 11 | 3 |
| 16 | 96 | 4 | | | 67 | 23 | 25 | 36 | 13 | 3 |
| 17 | 96 | 3 | 1 | | 68 | 22 | 25 | 35 | 14 | 4 |
| 18 | 95 | 4 | 1 | | 69 | 21 | 25 | 34 | 16 | 4 |
| 19 | 94 | 5 | 1 | | 70 | 20 | 25 | 34 | 17 | 4 |
| 20 | 94 | 4 | 2 | | 71 | 19 | 25 | 32 | 20 | 4 |
| 21 | 94 | 4 | 2 | | 72 | 17 | 25 | 32 | 22 | 4 |
| 22 | 93 | 5 | 2 | | 73 | 16 | 25 | 31 | 24 | 4 |
| 23 | 93 | 5 | 2 | | 74 | 14 | 25 | 31 | 25 | 5 |
| 24 | 92 | 6 | 2 | | 75 | 13 | 25 | 29 | 28 | 5 |
| 25 | 92 | 6 | 2 | | 76 | 11 | 25 | 28 | 31 | 5 |
| 26 | 91 | 7 | 2 | | 77 | 10 | 25 | 27 | 32 | 6 |
| 27 | 90 | 8 | 2 | | 78 | 8 | 24 | 28 | 34 | 6 |
| 28 | 90 | 7 | 3 | | 79 | 6 | 24 | 28 | 36 | 6 |
| 29 | 89 | 8 | 3 | | 80 | 4 | 24 | 27 | 38 | 7 |
| 30 | 88 | 9 | 3 | | 81 | 2 | 24 | 27 | 40 | 7 |
| 31 | 86 | 11 | 3 | | 82 | | 24 | 27 | 41 | 8 |
| 32 | 85 | 12 | 3 | | 83 | | 22 | 26 | 43 | 9 |
| 33 | 84 | 12 | 4 | | 84 | | 20 | 26 | 44 | 10 |
| 34 | 83 | 13 | 4 | | 85 | | 16 | 26 | 47 | 11 |
| 35 | 81 | 15 | 4 | | 86 | | 13 | 26 | 49 | 12 |
| 36 | 80 | 16 | 4 | | 87 | | 9 | 26 | 51 | 14 |
| 37 | 78 | 17 | 5 | | 88 | | 6 | 26 | 52 | 16 |
| 38 | 76 | 18 | 6 | | 89 | | 2 | 26 | 54 | 18 |
| 39 | 74 | 20 | 6 | | 90 | | | 25 | 55 | 20 |
| 40 | 72 | 21 | 7 | | 91 | | | 22 | 56 | 22 |
| 41 | 69 | 23 | 8 | | 92 | | | 18 | 58 | 24 |
| 42 | 66 | 25 | 8 | 1 | 93 | | | 13 | 61 | 26 |
| 43 | 64 | 26 | 9 | 1 | 94 | | | 9 | 62 | 29 |
| 44 | 60 | 30 | 8 | 2 | 95 | | | 4 | 64 | 32 |
| 45 | 58 | 31 | 9 | 2 | 96 | | | | 64 | 36 |
| 46 | 54 | 34 | 10 | 2 | 97 | | | | 60 | 40 |
| 47 | 50 | 36 | 12 | 2 | 98 | | | | 57 | 43 |
| 48 | 47 | 38 | 13 | 2 | 99 | | | | 51 | 49 |
| 49 | 44 | 40 | 13 | 3 | 100 | | | | 48 | 52 |
| 50 | 41 | 42 | 14 | 3 | | | | | | |

In order to facilitate practical use of the method, mimeographed work sheets containing a schematic diagram of the combination process, as well as other pertinent information, were prepared. Figure 7 illustrates a portion of this work sheet, and figures 8 and 9 are examples of forecasts made using the method.

## FORECAST ACCURACY

Tables 2, 3, and 4 are contingency tables showing forecast and observed precipitation amounts for original data, independent test data, and actual forecasts made at the Los Angeles Forecast Center during the same period as the test data. Objective forecasts for both original and test data were made from computed values of $Y_2$ as shown in the table in the work sheet, figure 7.

TABLE 2.—*Contingency table showing verification of objective forecasts for original data (October–March 1946–47 and 1947–48)*

| | | Forecast precipitation (inches) | | | | | |
|---|---|---|---|---|---|---|---|
| | | No rain | 0.01–0.15 | 0.16–0.49 | 0.50–1.50 | Over 1.50 | Total |
| Observed precipitation (inches) | No rain | 280 | 13 | 5 | 0 | 0 | 298 |
| | 0.01–0.15 | 15 | 9 | 1 | 3 | 0 | 28 |
| | 0.16–0.49 | 7 | 2 | 4 | 2 | 0 | 15 |
| | 0.50–1.50 | 0 | 4 | 2 | 9 | 0 | 15 |
| | Over 1.50 | 0 | 0 | 1 | 0 | 1 | 2 |
| Total | | 302 | 28 | 13 | 14 | 1 | 358 |

Percentage correct: $\frac{303}{358}$=0.85; Skill score*: $\frac{303-255}{358-255}$=0.47

*The skill score is defined as the ratio of correct forecasts to total forecasts exceeding those which would be correct if the same forecasts were distributed by chance. The formula for the skill score ($S$) is thus:

$$S=\frac{C-E}{T-E}$$

where $C$=number of correct forecasts, $T$=total number of forecasts, $E$=number of forecasts expected correct due to chance. The theory and procedure involved in computation of $E$ may be found in almost any statistical text.

Weather Bureau Airport Station
Los Angeles, Calif.

OBJECTIVE PRECIPITATION FORECAST FOR PERIOD 6 TO 36 HOURS FOLLOWING MAP TIME

Date _____

Map time _____ PST

$\Delta P_{SFO-LAX}$ _____
$H_{700}$ _____
(fig. 1) $X_1$ _____

$\Delta P_{LAX-PHX}$ _____
$P_{SFO}$ _____
(fig. 2) $X_2$ _____

(fig. 4) $Y_1$ _____

$T_{700}$ _____
$D_{SDB}$ _____
(fig. 3) $X_3$ _____

(fig. 5) $Y_2$ _____

| When $Y_2$ is: | Most probable amount of rain to be forecast is: | Relative probability, % (from table 1) |
|---|---|---|
| 0 - 49 | No rain | |
| 50 - 62 | .01 - .15 | |
| 63 - 75 | .16 - .49 | |
| 76 - 99 | .50 - 1.50 | |
| 100 | 1.51 or more | |

FIGURE 7.—Sample of forecasting work sheet showing method of combining variables, and giving most probable rain amounts to be forecast for categorical values of $Y_2$. See page 115 for definitions of symbols.

TABLE 3.—*Contingency table showing verification of objective forecasts for independent data (October–March 1944–45 and 1945–46)*

| | | Forecast precipitation (inches) | | | | | |
|---|---|---|---|---|---|---|---|
| | | No rain | 0.01–0.15 | 0.16–0.49 | 0.50–1.50 | Over 1.50 | Total |
| Observed precipitation (inches) | No rain | 273 | 11 | 5 | 1 | 0 | 290 |
| | 0.01–0.15 | 16 | 4 | 6 | 3 | 0 | 29 |
| | 0.16–0.49 | 3 | 4 | 7 | 1 | 0 | 15 |
| | 0.50–1.50 | 6 | 2 | 4 | 9 | 0 | 21 |
| | Over 1.50 | 0 | 0 | 1 | 0 | 0 | 1 |
| Total | | 298 | 21 | 23 | 14 | 0 | 356 |

Percentage correct: $\frac{293}{356}$=0.82; Skill score: $\frac{293-246}{356-246}$=0.43

TABLE 4.—*Contingency table showing verification of actual forecasts, PFR system (October–March 1944–45 and 1945–46)*

| | | Forecast precipitation (cumulative code number) | | | | | |
|---|---|---|---|---|---|---|---|
| | | 0 | 1 | 2 | 3 | ≥4 | Total |
| Observed precipitation (cumulative code number) | 0 | 244 | 15 | 4 | 4 | 2 | 269 |
| | 1 | 15 | 6 | 4 | 2 | 2 | 29 |
| | 2 | 8 | 3 | 2 | 0 | 2 | 15 |
| | 3 | 2 | 3 | 2 | 2 | 7 | 16 |
| | ≥4 | 2 | 4 | 3 | 8 | 18 | 35 |
| Total | | 271 | 31 | 15 | 16 | 31 | 364 |

Percentage correct: $\frac{272}{364}$=0.75; Skill score: $\frac{272-207}{364-207}$=0.41

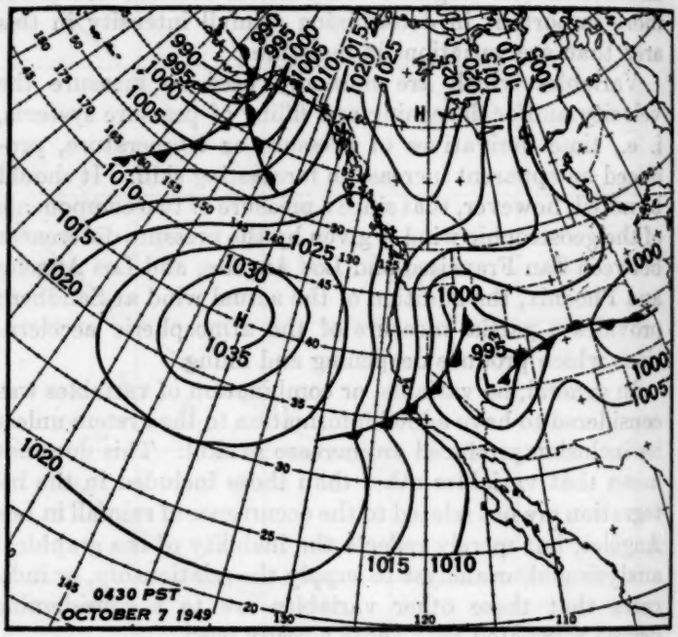


$\Delta P_{SFO-LAX}$ 3.7
$H_{700}$ 9860
$X_1$ 28

$\Delta P_{LAX-PHX}$ 5.1
$P_{SFO}$ 1012.2
$X_2$ 22

$Y_1$ 31

$T_{700}$ 6
$D_{SDB}$ NW
$X_3$ 20

$Y_2$ 30

| Relative Probability (From table 1) | |
|---|---|
| No Rain | .88 |
| .01 - .15 | .09 |
| .16 - .49 | .03 |
| .50 - 1.50 | - |
| Over 1.50 | - |

MOST PROBABLE AMOUNT FORECAST: NO RAIN

ACTUAL RAINFALL: NO RAIN

FIGURE 8.—Example of surface weather map and objective forecast for threatening frontal situation which produced no rain at Los Angeles.

The PFR forecast verifications (table 4) are for the same period and, except for code number "1," which at that time included rainfall of a trace to 0.15 inch, instead of the interval 0.01 to 0.15 inch, the code numbers cover the same categories as the independent forecasts in the previous table. However, it should be noted that the PFR forecasts were made for three separate time intervals during the forecast period; i. e., this afternoon, tonight, and tomorrow. In the above table, the code numbers (0 to 4) for the three time intervals were simply added and verifications were based on these cumulated values. Since it is difficult to say whether or not either of the forecasting methods might have been favored by this procedure, the justification for comparing the independent objective forecast and the actual PFR forecast scores is somewhat doubtful.

## COMPARISON OF OBJECTIVE AND ACTUAL FORECASTS

In order to make a more valid comparison of the objective and actual forecasts, as well as to determine, if possible, whether or not conventional forecasting methods are able to add significantly to the accuracy of the objective system, a comprehensive test was arranged for the winter (October–March) of 1949–50. Two forecasts were made each day, by two different forecasters, the first being made at 0700 PST and the second at 0800 PST. In the first instance, the forecaster had available all information used in the objective system including the computed objective forecast and analyzed 0430 PST surface map. The second forecaster had the added advantage of being able to check on the data for the following three-hourly (0730 PST) surface chart.

Forecasts were made and verified for the same rainfall categories, and for the same period as the objective system. Furthermore, in order to minimize the areal variation produced by a single station rainfall measurement, the amounts were verified by using unweighted means of the precipitation recorded at three weather stations in the Los Angeles Basin; i. e., Los Angeles Airport, Los Angeles City Office, and Burbank Airport.

Results of this test are given in tables 5, 6, and 7.

Although the skill shown by the objective forecast is greater than for either of the other forecasts, a statistical (Chi-square) test indicates that, at the 5 percent significance level, the differences in frequency distributions for the three contigency tables may be assumed due to chance variations. This means that there is no significant difference in the accuracy of the three forecasts,

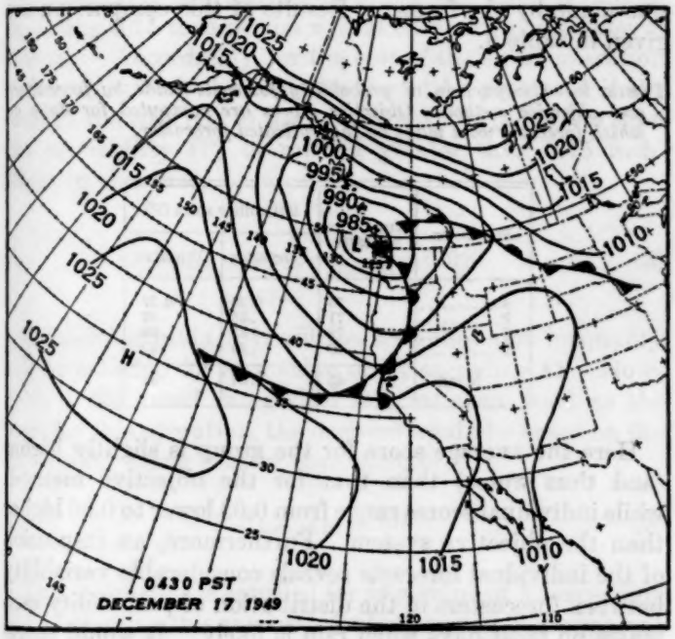


$\Delta P_{SFO-LAX}$ -6.1
$H_{700}$ 9790
$X_1$ 69
$\Delta P_{LAX-PHX}$ 0.0
$P_{SFO}$ 1009.8
$X_2$ 60
$Y_1$ 76
$T_{700}$ 0
$D_{SDB}$ SSW
$X_3$ 64
$Y_2$ 76

| Relative Probability (From table 1) | |
|---|---|
| No Rain | .11 |
| .01 - .15 | .25 |
| .16 - .49 | .28 |
| .50 -1.50 | .31 |
| Over 1.50 | .05 |

MOST PROBABLE AMOUNT FORECAST: .50 - 1.50 in.

ACTUAL RAINFALL: 1.15 in.

FIGURE 9.—Example of surface weather map and objective forecast for frontal situation which produced over an inch of rain at Los Angeles.

TABLE 5.—*Contingency table showing verification of objective forecasts (Oct. 1, 1949—March 31, 1950)*

| | | Forecast precipitation (inches) | | | | | |
|---|---|---|---|---|---|---|---|
| | | No rain | 0.01–0.15 | 0.16–0.49 | 0.50–1.50 | Over 1.50 | Total |
| Observed precipitation (inches) | No rain | 145 | 4 | 2 | 0 | 0 | 151 |
| | 0.01–0.15 | 6 | 3 | 2 | 2 | 1 | 14 |
| | 0.16–0.49 | 3 | 0 | 4 | 0 | 0 | 7 |
| | 0.50–1.50 | 2 | 0 | 4 | 3 | 0 | 9 |
| | Over 1.50 | 0 | 0 | 1 | 0 | 0 | 1 |
| Total | | 156 | 7 | 13 | 5 | 1 | *182 |

Percentage correct: $\frac{155}{182}$=0.85; Skill score: $\frac{155-131}{182-131}$=0.47

*Differences in total forecasts in Tables 5, 6, and 7 are due to a few missing data in the latter two tabulations. However, a computation of percentage of correct forecasts and skill scores for those days for which information was available for all three forecasts resulted in exactly the same scores as those listed.

TABLE 6.—*Contingency table showing verification of actual forecasts made at 0700 PST (Oct. 1, 1949—March 31, 1950)*

| | | Forecast precipitation (inches) | | | | | |
|---|---|---|---|---|---|---|---|
| | | No rain | 0.01–0.15 | 0.16–0.49 | 0.50–1.50 | Over 1.50 | Total |
| Observed precipitation (inches) | No rain | 140 | 9 | 0 | 0 | 0 | 149 |
| | 0.01–0.15 | 7 | 2 | 2 | 2 | 1 | 14 |
| | 0.16–0.49 | 2 | 2 | 2 | 1 | 0 | 7 |
| | 0.50–1.50 | 3 | 2 | 1 | 2 | 0 | 8 |
| | Over 1.50 | 0 | 0 | 0 | 1 | 0 | 1 |
| Total | | 152 | 15 | 5 | 6 | 1 | 179 |

Percentage correct: $\frac{146}{179}$=0.82; Skill score: $\frac{146-128}{179-128}$=0.35

TABLE 7.—*Contingency table showing verification of actual forecasts made at 0800 PST (Oct. 1, 1949–Mar. 31, 1950)*

| | | Forecast precipitation (inches) | | | | | |
|---|---|---|---|---|---|---|---|
| | | No. rain | 0.01–0.15 | 0.16–0.49 | 0.50–1.50 | Over 1.50 | Total[1] |
| Observed precipitation (inches) | No rain | 142 | 8 | 0 | 0 | 0 | 150 |
| | 0.01–0.15 | 8 | 1 | 4 | 1 | 0 | 14 |
| | 0.16–0.49 | 3 | 2 | 1 | 1 | 0 | 7 |
| | 0.50–1.50 | 1 | 0 | 5 | 3 | 0 | 9 |
| | Over 1.50 | 0 | 0 | 1 | 0 | 0 | 1 |
| Total | | 154 | 11 | 11 | 5 | 0 | 181 |

Percentage correct: $\frac{147}{181}$=0.81; Skill score: $\frac{147-129}{181-129}$=0.35

and confirms the previous comparison made between the independent test sample, table 3, and the actual PFR forecasts, table 4.

Any attempt to generalize on the above results in the light of their possible effect on current forecasting procedures is beyond the scope of this discussion. Here it is desired only to suggest that, in this case at least, the numerical forecasting technique produced results which were at least as accurate as, and were not improved upon by, conventional methods. At the same time, by presenting the forecast in terms of probabilities, the numerical method provided a measure of the reliability of each prediction.

## PROBABILITY DISTRIBUTION

Occasional attempts have been made to provide probability forecasts in the past, notably by Besson [11] in France, Cooke [12] in Australia, and Hallenbeck [13] in the United States. Except in the case of Besson's studies, however, all such forecasts were based upon subjective estimates of the probability distribution and were consequently dependent upon the individual forecasters' experience, skill, and certain psychological factors. The numerical forecasts discussed here are not subject to such influences and, at the same time, are apparently quite as accurate as those issued by conventional methods.

It should be noted, however, that the accuracy of the categorical forecasts may not necessarily reflect the precision of the probability estimates. A method for evaluating the latter, suggested recently by G. W. Brier [14], is described briefly below. If the probability estimates are placed in a contingency table as follows,

| | | Forecasts | | |
|---|---|---|---|---|
| | | 1 | 2 ... | n |
| Forecast events | 1 | $p_{11}$ | $p_{12}$ | $p_{1n}$ |
| | 2 | $p_{21}$ | $p_{22}$ | $p_{2n}$ |
| | r | $p_{r1}$ | $p_{r2}$ | $p_{rn}$ |

where the $p_{ij}$ are the forecast probabilities in the $i$th row and $j$th column, then the reliability of the forecasts ($P$) may be defined as,

$$P=\frac{1}{n}\sum_{i=1}^{r}\sum_{j=1}^{n}(p_{ij}-E_{ij})^2 \qquad (1)$$

where $E_{ij}$ is 0 when the forecast event does not occur, and $E_{ij}$ is 1 when the forecast event does occur.

Here the $E_{ij}$ are the actual, or observed, probabilities so essentially what is done in the above formula is to compute the mean of the squares of the differences between the forecast probability distribution and the observed distribution. If the forecast events are mutually exclusive, the reliability score has a range of from zero to two. Since one would like to have the difference as small as possible, a good score is one which is small.

A rough check on the consistency of probability forecasts made by several individual forecasters in competition with the objective system was carried on at Los Angeles for a short period during the past winter. Due to schedule differences, days off, etc., forecasters' probability estimates were not made every day; consequently the comparison has been made between forecasters' scores and objective scores for only those days on which a forecast was made by the former. Results of this comparison are given in table 8.

TABLE 8.—*Comparison of probability forecasts made by forecasters and objective method. Objective scores are computed for days on which forecasts were made by the indicated forecaster*

| Forecaster | Number of forecasts | Reliability score (P) | |
|---|---|---|---|
| | | Forecaster | Objective |
| A | 75 | 0.26 | 0.27 |
| B | 71 | .35 | .32 |
| C | 72 | .35 | .29 |
| D | 40 | .39 | .42 |
| Mean | 65 | .34 | .31 |

Here the average score for the group is slightly higher (and thus worse) than that for the objective method, while individual scores range from 0.03 lower to 0.06 higher than the objective system. Furthermore, an inspection of the individual forecasts reveals considerable variability between forecasters in the distribution of probability estimates on most days when rain is likely. It would therefore appear that in this case a more reliable estimate of the error frequency distribution for each forecast may be obtained from the objective method.

## USE OF PROBABILITY FORECASTS

The usefulness of the reliability measurement provided by the probability forecast may be brought out by applying the well-known principle of calculated risk. As is true of statistical techniques in general, this principle requires that the decisions based on the forecasts be applied only to repetitive operations. Furthermore, the user in this case should have available complete information concerning the cost of each operation as well as an estimate of the

contingent gain or loss which will result if the forecast events do not occur. Then, in order to keep the cost of the series of operations at a minimum, decisions should be made by balancing the probability of occurrence of the forecast event against the ratio of the cost to the contingent gain or loss. This means that the usual categorical forecast may not be the most valuable prediction for all recipients since it is aimed at providing a forecast to suit the "average" user and is quite properly based (either subjectively or objectively) on the probability of occurrence being greater or less than 0.50.

Some uses of probability forecasts have already been discussed briefly by Brier [15] and Price [16] for certain special types of weather problems. However, it may be of interest to provide an example of how the rainfall forecasts described herein could be used to good advantage. Consider, therefore, a hypothetical Los Angeles construction company which is engaged in making a series of concrete pours during the winter months. The company finds that it will cost about $400 to protect the concrete each time, but that damage of $5,000 will result if rainfall exceeding 0.15 inch occurs within 36 hours of the time of pouring. Accordingly, for the cost of the entire operation to be minimized, the concrete should be protected if the ratio of the cost (C) to the contingent loss (L) is less than the probability (P) of rainfall greater than 0.15 inch. Thus, in this case,

$$P_{(\text{rain}>0.15)} > \frac{C}{L} = \frac{400}{5000} = 0.08 \qquad (2)$$

Consulting table 1, it will be seen that this inequality will be satisfied for any value of $Y_2$ exceeding 41. However, if the usual categorical forecast were used as the basis for this operation, the decision would be based on the probability being greater than 0.50, or,

$$P_{(\text{rain}>0.15)} > .50 \qquad (3)$$

This inequality is satisfied for any value of $Y_2$ exceeding 66. Accepting this as a basis for his decision, it is apparent that the contractor would not protect his concrete often enough.

In order to make this point clear, the comparison given below has been made of the cost of carrying on this operation throughout the past winter season (October 1, 1949–March 31, 1950) for several alternative procedures. Here, for the sake of simplicity, it is assumed that the contractor operates every day during the period (182 days).

| | *Total cost plus loss* |
|---|---|
| *Case I.*—The contractor obtains no forecast at all and takes no protective measures. Since there were 17 days with rain exceeding 0.15 inch during the period, the loss is $5,000 per day for 17 days | $85, 000 |
| *Case II.*—The contractor obtains no forecast but takes protective measures every day. He thus sustains no loss, but the cost is $400 per day for 182 days | 72, 800 |
| *Case III.*—The contractor uses climatological expectancy as a basis for the operation, taking protective measures only during the period when this expectancy is greater than 0.08. For Los Angeles this requires protection from December 11 until March 25 and no protection before or after that period. In this case the contractor would take protective measures on 105 days and would sustain a loss on 4 days | $62, 000 |
| *Case IV.*—The contractor uses "persistence"; i. e., takes protective measures on all days following a day with measurable rainfall and provides no protection on other days. This would require protection on 31 days and the contractor would suffer loss on 5 days | 37, 400 |
| *Case V.*—The contractor obtains a forecast designed for the "average" user and thus based on equation (3) above. Using the objective probability estimates, this would require protective measures on 19 days, and the contractor would suffer loss on 5 days | 32, 600 |
| *Case VI.*—The contractor obtains a forecast designed for his particular operation and thus based on equation (2). Using the objective probability estimates, this would require protective measures on 35 days, and the contractor would suffer loss on 2 days | 24, 400 |

An inspection of these figures reveals that, although the contractor in using the "average" forecast, Case V, would reduce the total cost of the operation below that for an operator using no forecast at all, or using climatological expectancy or persistence, the least total expenditure would result from the use of the probability forecast. This illustrates the advantage of the probability estimate and reveals the inherent danger in any categorical forecast where the user is not provided with, or does not make use of a measure of the reliability of the prediction. In the above example, only the objective probability forecasts have been considered, although probability estimates might also be made by the forecaster from a subjective evaluation of the meteorological situation. For some purposes where adequate numerical techniques are not available, such subjective probability forecasts undoubtedly could be used to good advantage.

## CONCLUSION

The gradual increase in the complexity of modern industrial, agricultural, military, and many other operations has resulted, during recent years, in a general desire for more accurate and increasingly specialized weather forecasts. The success with which such requirements can be met is of course dependent largely upon basic progress in the science of meteorology in general. At present, however, many of the physical relationships involved in weather forecasting are obscure, and of those that are understood a large number are mathematically indeterminate. Whether or not statistical techniques may be used to help in the development of a better physical understanding of the weather is beyond the scope of this discussion. It is desired here only to point out the usefulness of such techniques in evaluating the magnitude of the indeterminacy, and to suggest a method for making use of that evaluation in a practical application.

## ACKNOWLEDGMENT

Much of the research work involved in this study was carried on in cooperation with the Department of Meteorology, University of California at Los Angeles and was under the joint supervision of Prof. Jacob Bjerknes, Chairman of the Department, and the writer. Research assistants at U. C. L. A. were R. Robert Rapp, David Smedley, J. K. Angell, and Mrs. C. K. Chen-Wei, and at the Los Angeles Forecast Center was Mrs. Gwendolyn McMeans. Many valuable suggestions were also contributed by Mr. A. K. Showalter and the forecast staff at the Los Angeles Forecast Center.

## REFERENCES

1. J. C. Thompson, "Progress Report on an Objective Rainfall Forecasting Research Program for the Los Angeles Area," U. S. Weather Bureau *Research Paper No. 25*, July 1946.
2. J. C. Thompson, R. R. Rapp and D. Smedley, *Second Progress Report on an Objective Rainfall Forecasting Program for the Los Angeles Area*, Dept. of Meteorology, University of California at Los Angeles, July 1947.
3. J. K. Angell and C. K. Chen, *Final Report on Objective Rainfall Forecasting Program for the Los Angeles Area*, Dept. of Meteorology, University of California at Los Angeles, May 1948.
4. G. W. Brier, "A Study of Quantitative Precipitation Forecasting in the T. V. A. Basin," U. S. Weather Bureau *Research Paper No. 26*, November 1946.
5. Samuel Penn, "An Objective Method for Forecasting Precipitation Amounts from Winter Coastal Storms for Boston," *Monthly Weather Review*, vol. 76, No. 8, August 1948, p. 149–161.
6. D. L. Jorgensen, "An Objective Method of Forecasting Rain in Central California During the Raisin-Drying Season," *Monthly Weather Review*, vol. 77, No. 2, February 1949, p. 31–46.
7. W. W. Dickey, "Estimating the Probability of a Large Fall in Temperature at Washington, D. C.," *Monthly Weather Review*, vol. 77, No. 3, March 1949, p. 67–78.
8. A. K. Showalter, "An Approach to Quantitative Forecasting of Precipitation," *Bulletin of the American Meteorological Society*, vol. 25, No. 4, April 1944, p. 137–142; No. 7, September 1944, p. 276–288.
9. U. S. Weather Bureau, "Revised Report on Maximum Possible Precipitation, Los Angeles Area, California," *Hydrometeorological Report No. 21B*, December 29, 1945.
10. A. K. Showalter, A. J. Knarr, and R. D. Fletcher, Committee Report on Quantitative Rainfall Forecasting, U. S. Weather Bureau, August 6, 1948. (Unpublished.)
11. Louis Besson, "Essai de Prevision Methodique du Temps," *Annales de L'Observatiore Municipal, Ville de Paris*, Tome VI, 1905, 473–495.
12. W. E. Cooke, "Forecasts and Verifications in Western Australia," *Monthly Weather Review*, vol. 34, No. 1, January 1906, p. 23–24.
13. C. Hallenbeck, "Forecasting Precipitation in Percentages of Probability," *Monthly Weather Review*, vol. 48, No. 11, November 1920, p. 645–647.
14. G. W. Brier, "Verification of Forecasts Expressed in Terms of Probability," *Monthly Weather Review*, vol. 78, No. 1, January 1950, p. 1–3.
15. G. W. Brier, "Verification of a Forecaster's Confidence and the Use of Probability Statements in Weather Forecasting," U. S. Weather Bureau *Research Paper No. 16*, February 1944.
16. Saul Price, "Thunderstorm Today?—Try a Probability Forecast," *Weatherwise*, vol. 2, No. 3, June 1949, p. 61–63.

# THE WEATHER AND CIRCULATION OF JULY 1950[1]

WILLIAM H. KLEIN

Extended Forecast Section, U. S. Weather Bureau

Washington, D. C.

July 1950 was a remarkably cool, cloudy, and rainy month in the eastern three-quarters of the United States. In most areas from the Rocky Mountain States to the Atlantic Coast temperatures were below normal (Chart I), skies were clear less than half the time (Chart IV), and precipitation was excessive (Chart V and inset). These conditions were most marked in the southern and central Plains States, in portions of which the negative departure of mean temperature from normal exceeded 6° F., the percentage of clear sky between sunrise and sunset was less than 20, and total rainfall was more than 8 inches greater than the normal amount. Considering the extent and intensity of the below normal temperatures, this month was the coolest July of the last 25 years in the United States east of the Continental Divide and probably just as cool as any July of the past 40 years.

The principal feature of the general circulation with which this weather can be associated is a mean trough in the constant pressure surfaces located through the Mississippi Valley at all levels of the troposphere from 700 mb. to 300 mb. (Charts IX to XI). The field of 700-mb. height anomaly drawn in figure 1 shows that this trough was deeper than normal and displaced well to the west of its normal position, which is along the Atlantic Coast. As a

[1] See Charts I–XI, following p. 133, for analyzed climatological data for the month.

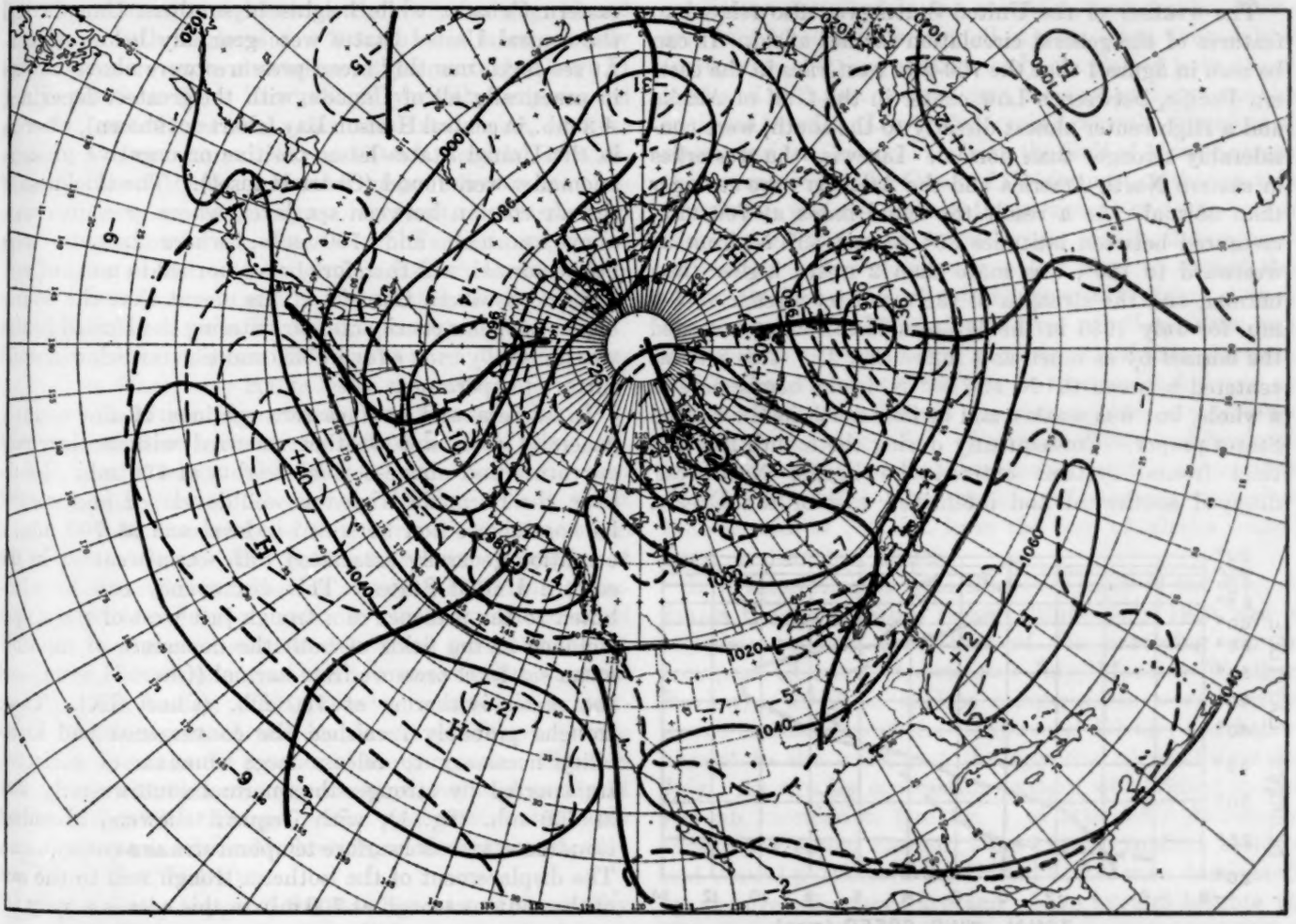


FIGURE 1.—Mean 700-mb. chart for the 30-day period July 1–30, 1950. Contours at 200-foot intervals are shown by solid lines, 700-mb. height departures from normal at 100-foot intervals by dashed lines with the zero isopleth heavier. Anomaly centers and contours are labeled in tens of feet. Minimum latitude trough locations are shown by heavy solid lines.

result cyclonic curvature prevailed in the circulation over the central part of the United States, where the warm High and subsidence aloft typical of the dust-bowl decade of the 1930's were conspicuous by their absence. Frequent showers and thunderstorms were favored by horizontal convergence, upward vertical motion, and instability in the vicinity of the trough, while daytime maximum temperatures were kept low by the large amount of associated cloudiness. Thus comparison of figure 1 with Charts I, IV, and V (inset) reveals in general a good agreement between the areas of cyclonic curvature and negative height anomaly at 700 mb. and the regions of much cloudiness, sub-normal temperature, and above-normal precipitation at the surface. Cloudiness and showers were also favored by large-scale convergence in a sharp inverted trough in the 1014-mb. mean isobar at sea level (Chart VI) in the central and southern Plains. In addition, large quantities of moisture were carried into this region from the Gulf of Mexico since sea level winds were more southeasterly than normal (Chart II inset).

The weather of the United States was also related to features of the general circulation farther afield. It can be seen in figure 1 that the 700-mb. westerlies in the eastern Pacific, between a Low center in the Gulf of Alaska and a High center almost directly to the south, were considerably stronger than normal. Likewise the westerlies in eastern North America and the Atlantic were stronger than normal. As a result the zonal index at 700 mb., measured between latitudes 35° N. and 55° N. from 0° westward to 180°, was more than 2 m/sec higher than normal, and the strength of the mean jet stream at 700 mb. for July 1950 in the Western Hemisphere exceeded the normal by as much as 3 m/sec (fig. 2). This jet was centered between 45° N. and 50° N. in the hemisphere as a whole, but was weaker and farther south in the United States proper. Consequently during the month five distinct frontal systems entered the Pacific Northwest, dropped southward and intensified east of the Divide,

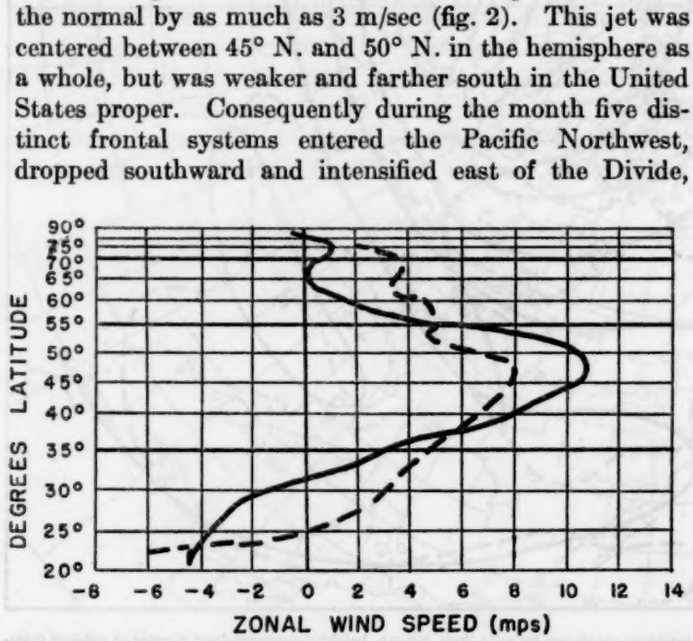


FIGURE 2.—Monthly mean 700-mb. geostrophic zonal wind speed profile in meters per second averaged from 0° westward to 180° longitude. Solid curve is for July 1950, dashed line is July normal.

and continued east-northeastward across the country into the Atlantic. Each was accompanied by widespread cloudiness and showers and followed by a surge of high pressure and cool maritime air from the north Pacific. These are not indicated in Charts II and III, however, because their continuity was obscured in the mountains of western North America due to the absence of a closed circulation.

After crossing the Continental Divide, these surges of cool Pacific air were reinforced by outbreaks of cool polar continental air from the Hudson Bay region. These outbreaks accompanied the movement of several anticyclones, from central Canada through the Dakotas, Minnesota, and the Lakes along tracks given in Chart II. Southward movement of cool Canadian air into the United States was facilitated by the fact that pressures relative to normal were generally higher in Canada than in the central United States. This was a type of blocking action which showed up at 700 mb. (fig. 1) as a westward protrusion of a strong positive height anomaly center over Greenland into northeastern Canada, while heights in southern Canada and the central United States were generally below normal. At sea level, monthly mean pressures were above normal in practically all of Canada, with the greatest departure, +3 mb., in central Hudson Bay (chart not shown), whereas in the United States lesser positive or negative pressure anomalies were found (Chart II inset). The thickness of the air column between sea level, where pressures were above normal, and 700 mb., where heights were below normal, was therefore below normal in most of central and southern Canada. This meant that the source region for polar continental air entering the United States was unusually cool, a favorable condition for below-normal surface temperatures.

In eastern and southeastern sections of the country generally cool, wet weather occurred with anticyclonic curvature and above-normal heights at 700 mb. Moreover, the Bermuda High was well developed and west of its normal position both at sea level and at 700 mb., a condition generally associated with warm weather in the eastern United States. This discrepancy can be attributed to the presence of a trough just west of the Appalachians in the fields of both the departure of monthly mean sea level pressure from normal (Chart II inset) and the mean isotherms at 700 mb. (Chart IX). These troughs probably furnished the convergence and instability necessary to release large amounts of moisture, transported by stronger-than-normal southwesterly flow at 700 mb. (fig. 1), with frequent showers, abundant cloudiness, and cool surface temperatures as a consequence. The displacement of the isotherm trough well to the east of the contour trough at 700 mb. in this area is a very unusual circumstance since contours and isotherms are nearly in phase on most monthly mean maps at upper levels. As a consequence the contour trough sloped to

the east with increasing elevation, at least from 700 to 300 mb., (compare Charts IX, X, and XI), temperatures at 700 mb. were below normal where heights were above normal in the Southeast, and the Bermuda High was cold and therefore quite weak in the upper troposphere. This anomalous nature of the Bermuda High is difficult to explain, but it probably contributed toward making this a generally cool, rainy July in the eastern United States.

The principal exceptions to the cool, wet regime east of the Divide were southeast Texas and portions of the Northeast. Chart I shows that temperatures were slightly above normal in coastal sections of New England and the Middle Atlantic States, and also in parts of New York, New Hampshire, and Vermont, while precipitation was generally deficient in these areas (Chart V inset) as well as in portions of Pennsylvania and Maryland. At Portland, Maine total precipitation for the month was less than half of the normal amount and only .01 inch more than the driest of record. This relatively warm, dry condition in the Northeast was associated with the fact that 700-mb. heights were above normal (fig. 1) and airflow at both sea level and 700 mb. was more westerly (and therefore more downslope) than normal (Chart II inset and Chart VI). The warm, dry weather experienced in southeast Texas was also associated with positive departures from normal of local 700-mb. height. In addition, review of the daily weather maps indicates the presence of a quasi-stationary polar front, oriented from northeast to southwest, across central Texas during a good deal of the month. Although it is difficult to detect this mean frontal zone on any of the monthly mean maps, it was primarily responsible for temperatures that were 3° above normal at Corpus Christi, but more than 2° below normal at Waco, only 200 miles to the north.

The fields of monthly mean sea level pressure (Chart VI) and its departure from normal (Chart II inset) show that southeasterly winds (see wind roses, Chart I) were stronger than normal throughout Florida. As a result cool ocean breezes caused below normal temperatures in most of the State. The greatest departure occurred at Miami, where the temperature averaged 1.9° below normal, the coolest July on record. On the west coast of Florida, however, temperatures were generally above normal as the easterly gradient flow weakened the normal westerly sea breeze. This probably resulted in a westward displacement of the sea breeze convergence zone normally found in the interior of the peninsula. Showers associated with this convergence zone produced nearly 14 inches of rainfall at Tampa, on the west coast, but directly across the peninsula at Melbourne, on the east coast, only 4 inches fell (Chart V).

As frequently happens, the weather west of the Rocky Mountain States was of quite a different character than that to the east. Chart I shows that temperatures were predominantly above the seasonal normal in Washington, Oregon, California, Nevada, and Arizona, with the greatest departure, 4.8°, at Red Bluff, Calif. This abnormal surface warmth was intimately related to the existence of a well-developed thermal low at sea level (Chart VI), in the center of which pressures were as much as 3 mb. below normal (Chart II inset), and to strong anticyclonic vorticity at 700 mb. (fig. 1). In addition airflow was more northeasterly than normal at sea level and northerly relative to normal at 700 mb., so that warming was favored by downslope winds and by abundant insolation (Chart IV). In coastal sections of northern California, Oregon, and Washington, on the other hand, temperatures averaged slightly below normal because of the predominance of strong sea breezes (see wind roses, Chart I) and stratus cloud conditions (Chart IV), induced by abnormal warmth in the interior valleys.

It is perhaps surprising that total rainfall during the month exceeded the normal amount throughout the southern half of California and most of Nevada, Utah, and Arizona since dry weather usually goes with the warm conditions described in the preceding paragraph. However, nearly all of this rain fell in a few days, from July 5 to 10, when a strong southeasterly circulation both at sea level and aloft, accompanying a tropical cyclone near the southern tip of the Lower California peninsula, transported moist maritime tropical air from the Gulf of Mexico across the mountains to the Coast of California. Although this circulation was not sufficiently persistent or recurrent to show up on the mean maps for the month, it produced sufficiently heavy showers in a few days to exceed the extremely low totals of rainfall normally observed in a month in the southwest desert area. Gulf moisture was not able to penetrate into northern California, Oregon, and Idaho, where precipitation was generally deficient as dry northeasterly flow at the surface and anticyclonic curvature aloft prevailed. Pacific moisture and frequent frontal passages produced excessive rainfall in western Washington due to the presence of stronger westerlies than normal at 700 mb. from the Gulf of Alaska southward, as described earlier.

It is interesting to note that over most of the United States the temperature regime during July 1950 was a complete reversal from that of the preceding month (compare Charts I of June and July, Monthly Weather Review). In June surface temperatures were mostly above normal east of the Continental Divide, and below normal to the west, just the opposite of conditions in July. An equally contrasting pattern was evident in the 700-mb. circulation (see fig. 1 of article by Aubert in Monthly Weather Review, June 1950). In June eastern and central portions of the United States were dominated by anticyclonic curvature and above normal heights at 700 mb., while the western third of the country was under the influence of a well-developed mean trough, just the opposite of the 700-mb. pattern in July.

# LOW MINIMUM TEMPERATURES IN NORTH CENTRAL UNITED STATES, JULY 13, AND 14, 1950

CHARLES M. LENNAHAN AND LEWIS C. NORTON

WBAN Analysis Center, U. S. Weather Bureau

Washington, D. C.

## INTRODUCTION

Unusually low temperatures occurred over the north central United States on July 13 and 14, 1950, with minima at some points equal to or below the lowest ever recorded during the month of July. They were the result of southward flow of cold air in the wake of a depression which moved across extreme southern Canada, the cooling being intensified by nighttime radiation in an extensive High which built up over the western Plains and North Central States. A feature of the synoptic situation, beginning some 5 days before the low temperature occurred, was the movement of an upper level pressure trough eastward from the Pacific across southern Canada and the northern United States, the trough deepening markedly along with strong southward flow of cold air on the 12th and 13th.

## SYNOPTIC CONDITIONS PRECEDING THE LOW TEMPERATURES

On July 8, a deep surface Low which had been moving eastward across the Pacific, was centered along the British Columbia coast and had begun to fill. By the 10th this surface Low had filled, but the upper Low at the 700-mb. level, while also filling, had maintained its identity and had continued to move slowly eastward. The position of the upper Low at 2200 EST on the 9th, off northern Vancouver Island, may be seen in figure 1.

On the 8th, colder air south of the surface Low began moving into western Washington and Oregon. It progressed eastward ahead of the upper Low, the upper Low marking roughly the center of the dome or tongue of colder air to the rear of the surface front. This surface cold front was later identified with developments accompanying the cold air outbreak over the northern Plains area, though the low temperatures occurred mainly in continental air.

Figure 2, for 2200 EST on the 10th, shows the upper level Low over British Columbia. It had moved eastward and filled slightly in 24 hours. Thereafter, it moved more rapidly eastward and deepened somewhat, being centered over Manitoba at 2200 EST on the 11th (fig. 3).

It is of interest to note the position of the tropopause at this time as indicated in figure 4. This figure shows the intersection of the tropopause with the 200-mb. level, the stratosphere being lower to the north and higher to the south of the intersection. At 2200 EST on the 11th, the intersection was bulged northward over Manitoba and western Ontario in accordance with the usual association of warm air with a high stratosphere. Over Montana the

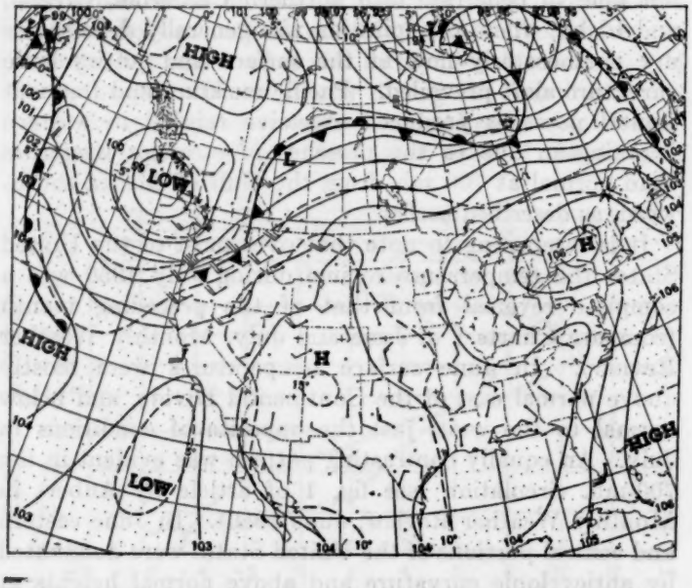


FIGURE 1.—700-mb. chart for 2200 EST, July 9, 1950. Contours (solid lines) at 100-foot intervals are labeled in hundreds of geopotential feet. Isotherms (dashed lines) are drawn for intervals of 5° C. Barbs on wind shafts are for wind speeds in knots (full barb for every 10 knots, half barb for every 5 knots, and pennant for every 50 knots).

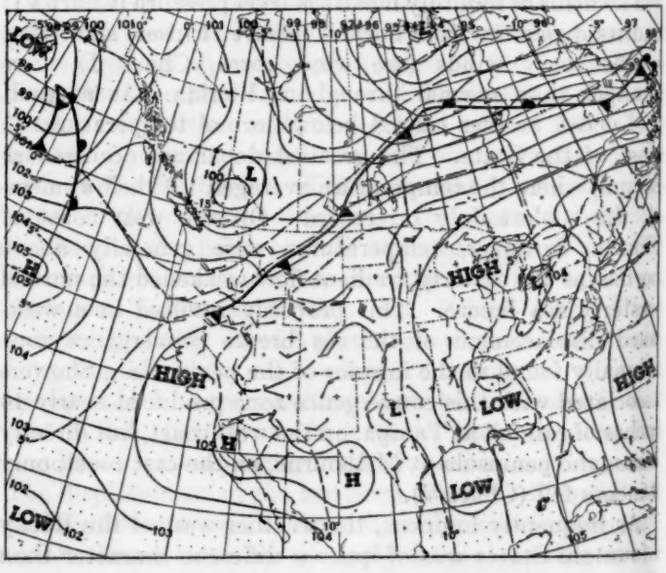


FIGURE 2.—700-mb. chart for 2200 EST, July 10, 1950.

intersection was pushing southward along with southward movement of cold air which may be seen at the 700-mb. level in figure 3. Subsequent changes in the configuration of the tropopause intersection are indicated in figure 4 at 24-hour intervals as the cold air progressed farther southward into the north central United States.

Figure 5 shows surface conditions at 0130 EST on the 11th, corresponding approximately in time to figure 2. The surface cold front had then reached the western Dakotas and colder continental air had begun to flow southward from the area west of Hudson Bay where, in turn, still colder air was being fed southward around a deep Low near the northern end of the bay. There was a weak Low along the front in the western Dakotas, and while it had not yet deepened appreciably, there had been an increase of pressure difference (previous surface charts not shown) between its center and the Rockies accompanying the increased southward flow of cold air into Montana.

The long north-south streamline from north of Hudson Bay to Montana, as indicated by the isobars in figure 5, provided some hint at that stage that the cold air north of the bay would later sweep southward into the central United States. While the cold front through the western Dakotas originally marked the leading edge of colder air from the Pacific, there was no clear demarcation, at the time of figure 5, between the maritime air and the colder continental air tending to replace it as the southward flow out of Canada was established.

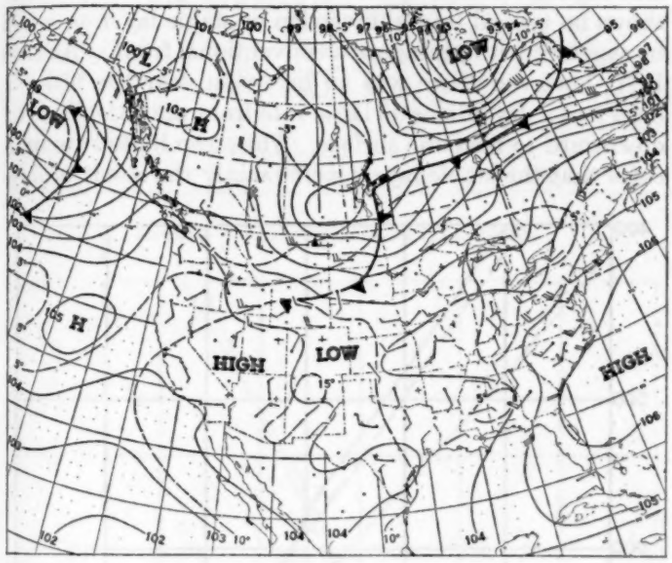


FIGURE 3.—700-mb. chart for 2200 EST, July 11, 1950.

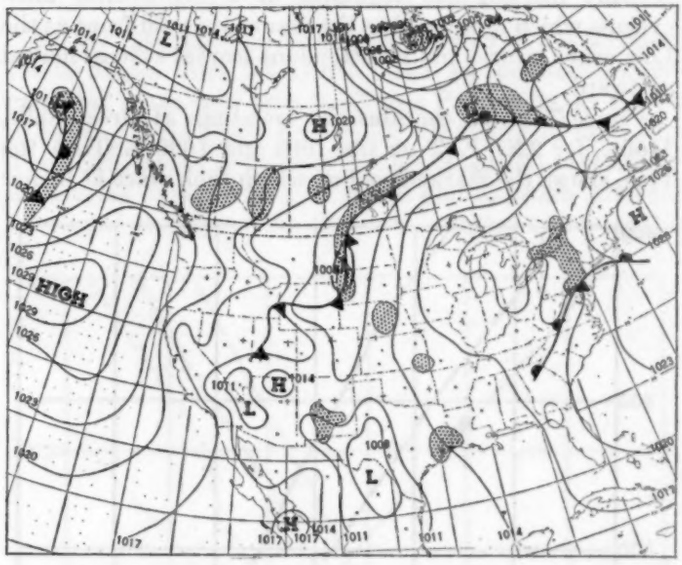


FIGURE 5.—Surface weather chart for 0130 EST, July 11, 1950. Shading indicates areas of active precipitation.

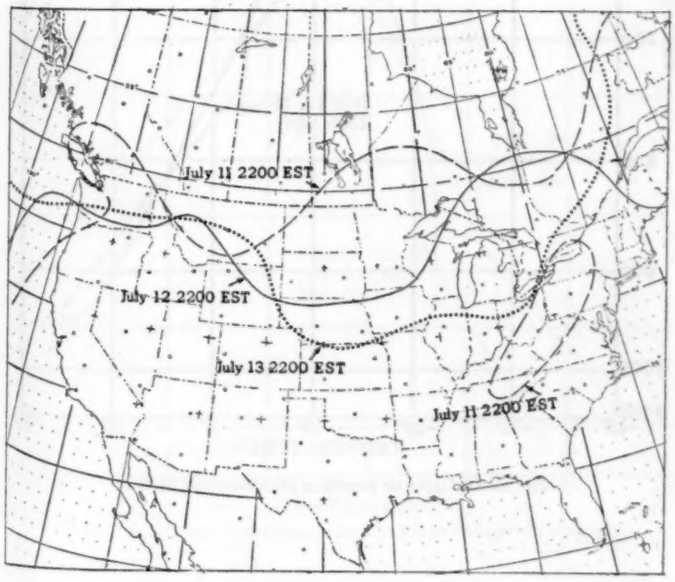


FIGURE 4.—Tropopause chart showing three positions of the intersection of the tropopause and the 200-mb. surface.

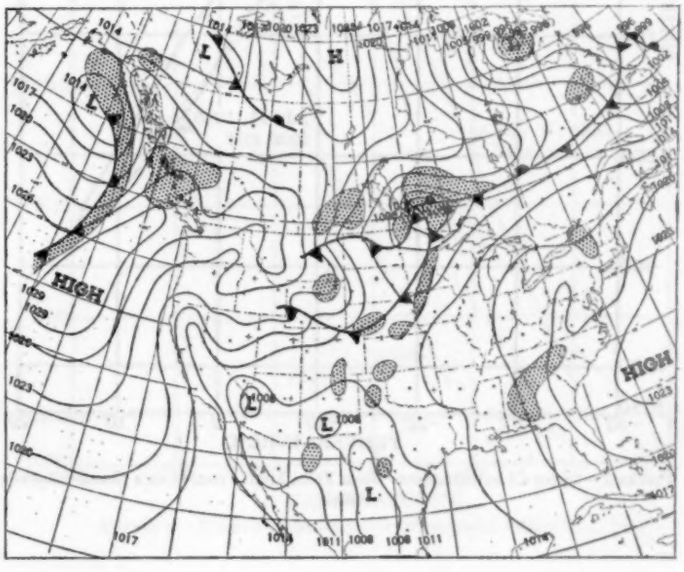


FIGURE 6.—Surface weather chart for 0130 EST, July 12, 1950. Shading indicates areas of active precipitation.

On the 11th, the surface wave along the cold front deepened along with intensified southward flow of cold air, its deepening perhaps accentuated by the accelerated eastward movement of the upper level Low. By the morning of the 12th (fig. 6) the surface Low was over extreme western Ontario with a central isobar of 1002 mb. The pressure difference between its center and the Continental Divide to the west had increased to over 25 mb. This large pressure difference was sufficient to insure that a substantial amount of colder air would flow into the northwestern Plains States, and later into the North Central States as the Low moved eastward. Another significant feature at that time (fig. 6) was the appearance of a high pressure ridge in southern Alberta and western Montana. It appeared to be an offshoot of the Pacific High, but actually marked the beginning of a continental anticyclone which developed to the rear of the cold front as the Low over Ontario and its attendant frontal system moved eastward.

Figure 7, which contains the soundings at Great Falls, Mont., for 2200 EST on the 10th and 1000 EST on the 11th, shows the marked cooling which took place at higher levels well after passage of the cold front from the Pacific. This cooling aloft was necessarily from the Pacific because trajectories at the higher levels were from a westerly direction. This meant that to the east of Great Falls cooling at low levels by the southward flow of continental air was being augmented aloft by cooler air off the Pacific, insuring that the cold outbreak would extend to great depths and thus not be subject to as much warming at the surface by insolation as would be the case with a shallow layer of cold air. This cooling aloft was also associated with arrival of the upper level cold trough as may be seen by inspection of figures 2 and 3.

Figure 8 shows two soundings at Bismarck, N. Dak., on the 12th, both taken after arrival of the cold air at both low and high levels. Because of the combination of low and high level cooling the first sounding, at 1000 EST, shows no typical frontal inversion or stable layer as would be expected with passage of a conventional front. At 2200 EST, however, there was an inversion near the 650-mb. level and a dry adiabatic lapse rate from the 735-mb. level downward to near the surface. The steep lapse rate indicates that the stable layers were mainly the result of day-

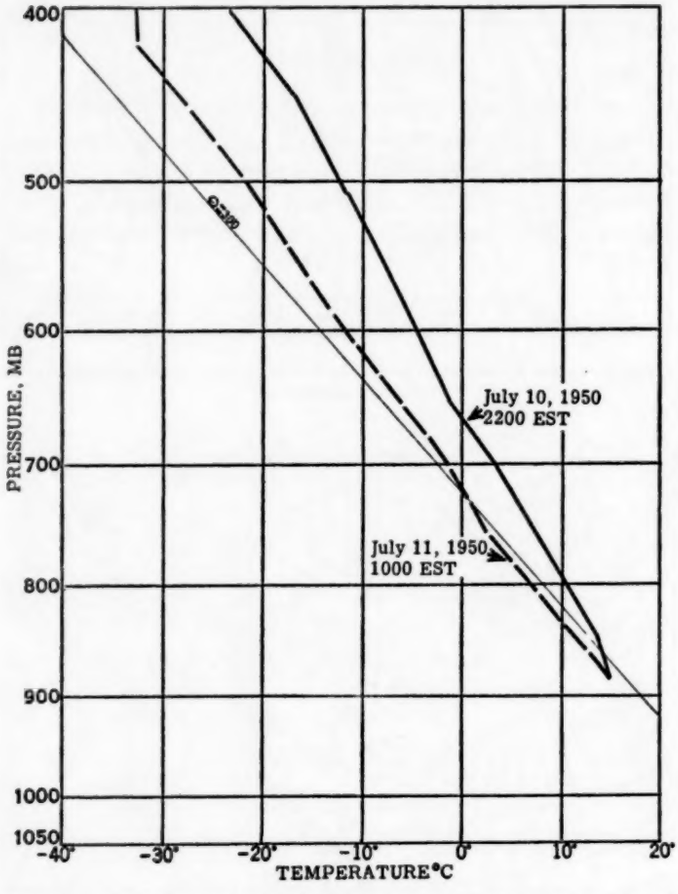


FIGURE 7.—Upper air soundings over Great Falls, Mont., plotted on a pseudo-adiabatic chart

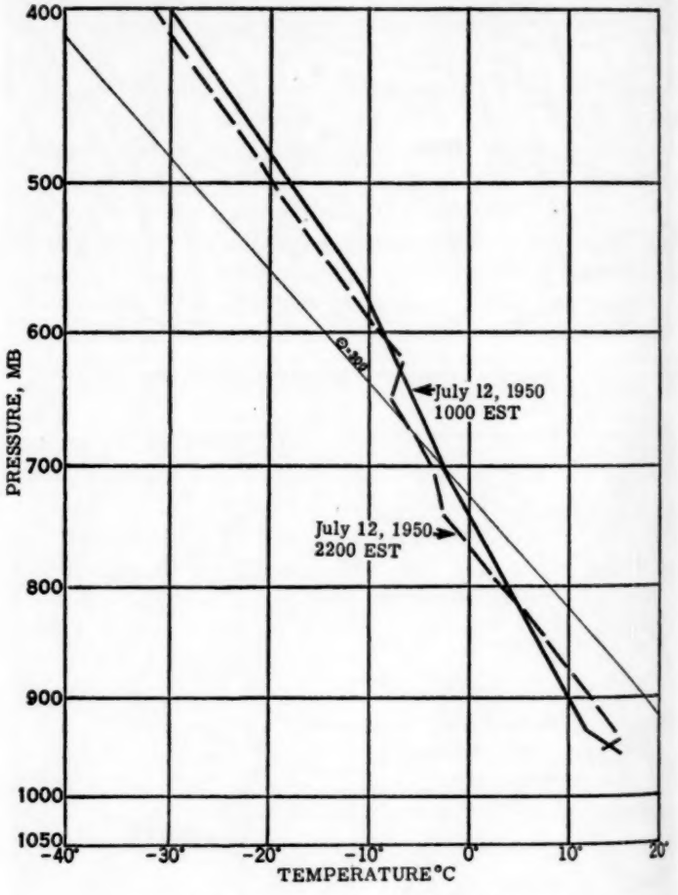


FIGURE 8.—Upper air soundings over Bismarck, N. Dak.

time turbulence, possibly accompanied by some subsidence at higher levels, though there was a slight net cooling above the stable layers. The depth of the turbulence layer was sufficient to allow only slow warming of the lower air by daytime heating during its southward movement.

An examination of the 700-mb. chart for 2200 EST of the 12th (fig. 9) shows that, at that level, Bismarck was near the confluence of airflows from the Pacific and from northern Canada. Temperatures aloft, where the airflow at 700 mb. was from the north, are illustrated by soundings from The Pas, Manitoba at 1000 EST on the 12th and Churchill, Manitoba, at 2200 EST on the 11th (fig. 10). The succession of temperature changes aloft at two northern United States stations are represented in figures 11 and 12 by soundings at 12 hour intervals at International Falls, Minn., and Sault Ste. Marie, Mich. The first sounding in each case was taken just prior to arrival of the colder air.

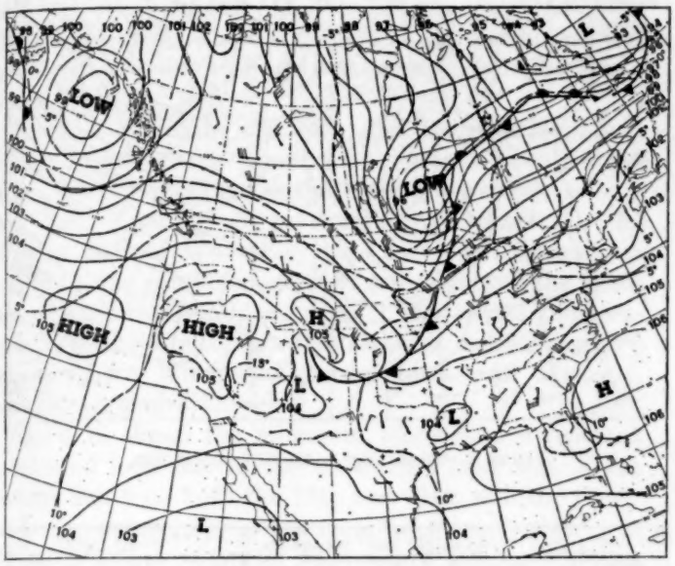


FIGURE 9.—700-mb. chart for 2200 EST, July 12, 1950.

## CONDITIONS DURING THE PERIOD OF LOW TEMPERATURES

On the 12th, the cold air outflow covered all the northern Plains States from the Great Lakes to the Rockies and extended southward into the Texas Panhandle, as shown in figure 13, the surface chart for 0130 EST of the 13th. The High, which in figure 6 (24 hours earlier) was barely discernible over western Montana and southern Alberta, developed rapidly on the 12th and in figure 13 covers the

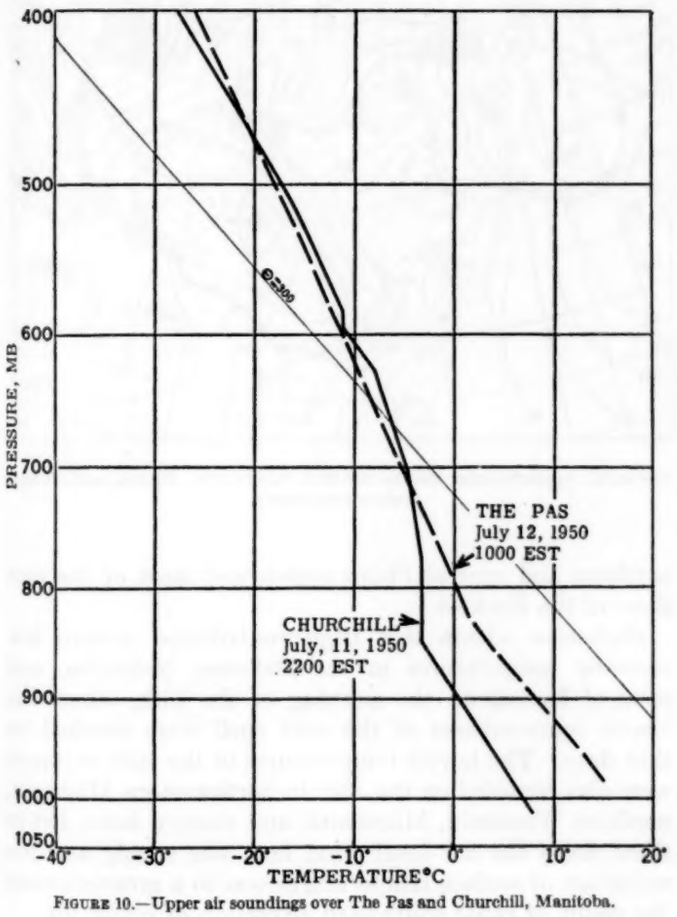


FIGURE 10.—Upper air soundings over The Pas and Churchill, Manitoba.

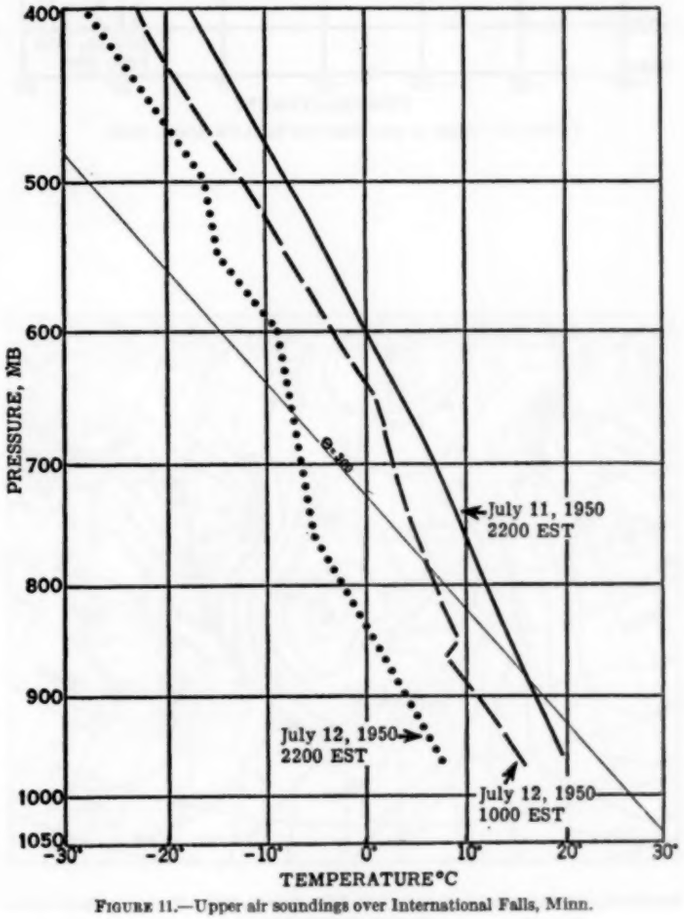


FIGURE 11.—Upper air soundings over International Falls, Minn.

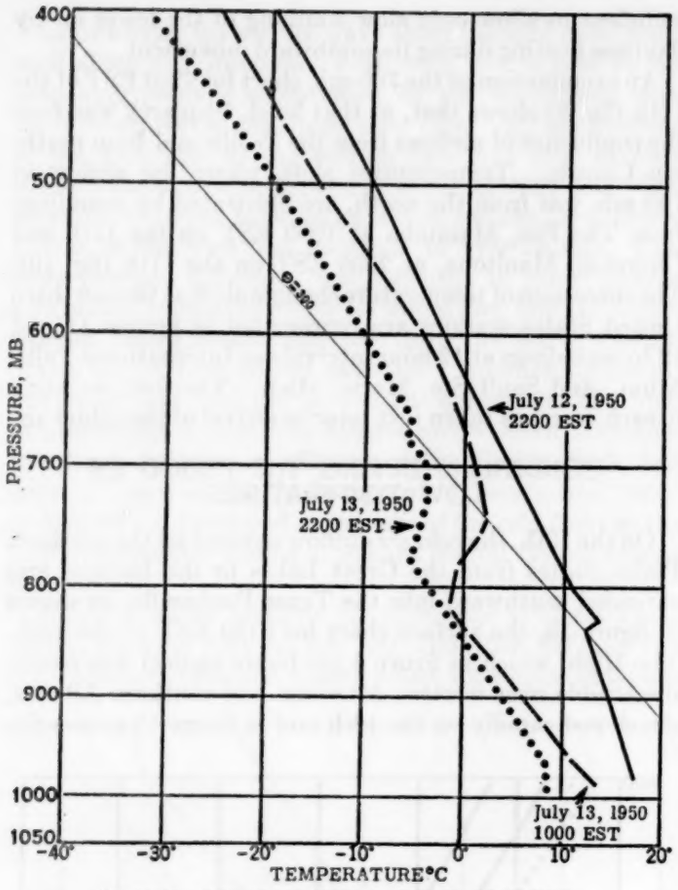


FIGURE 12.—Upper air soundings over Sault Ste. Marie, Mich.

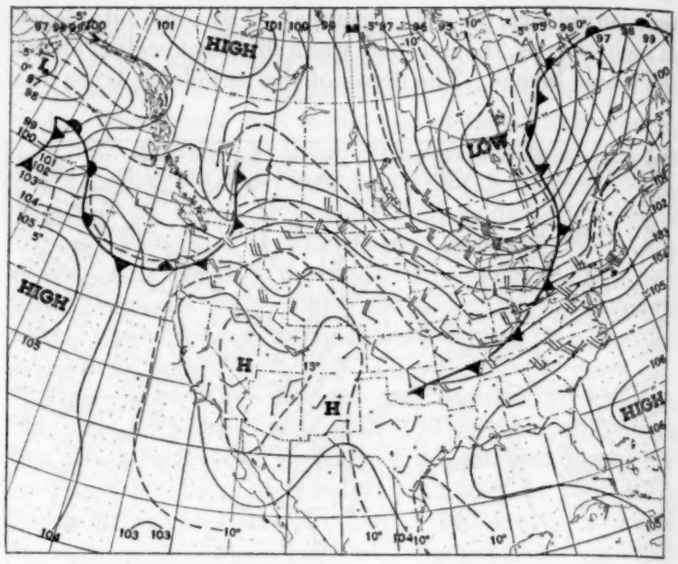


FIGURE 14.—700-mb. chart for 2200 EST, July 13, 1950.

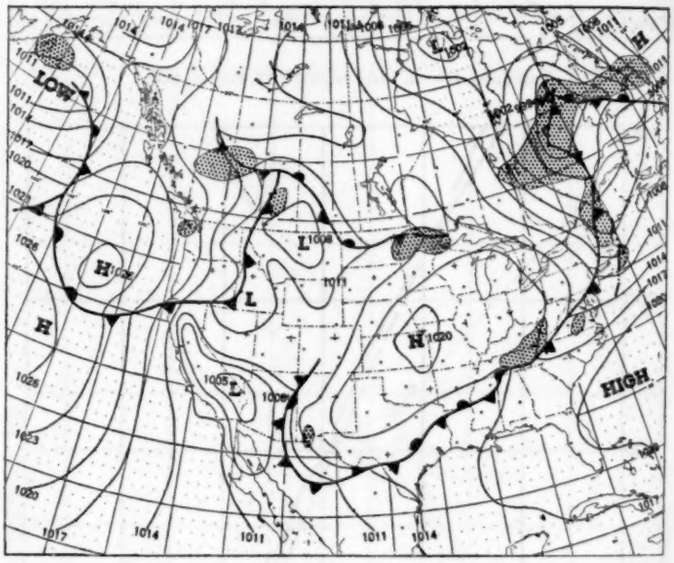


FIGURE 15.—Surface weather chart for 0130 EST, July 14, 1950. Shading indicates areas of active precipitation.

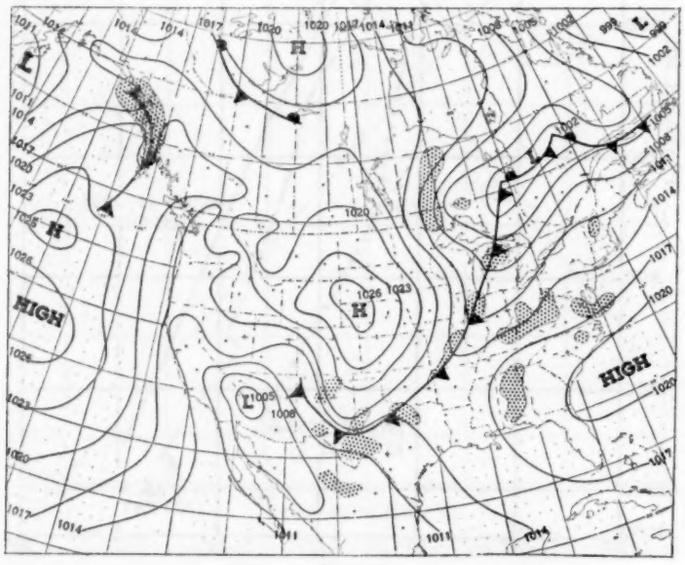


FIGURE 13.—Surface weather chart for 0130 EST, July 13, 1950. Shading indicates areas of active precipitation.

northern and central Plains region and most of the east slope of the Rockies.

Radiation within this High contributed toward low morning temperatures in the Dakotas, Nebraska, and most of Kansas on the morning of the 13th, where the lowest temperatures of the cold spell were reached on that date. The lowest temperatures of the cold outbreak were also recorded on the 13th in northwestern Michigan, northern Wisconsin, Minnesota, and western Iowa, but in these areas the low-level wind flow was strong and the reduction of surface temperatures was to a greater extent the result of rapid southward advection of colder air.

On the 13th, warmer air began to move in aloft over the northwestern Plains States, indicating a probable trend toward higher minimum temperatures over that area by the morning of the 14th. This advection of warmer air aloft is shown in figure 14, the 700-mb. chart for 2200 EST on the 13th, where transport of warmer air is indicated west of a line through northeastern Minnesota and central Iowa.

On the morning of the 14th (fig. 15), the High had become more extensive and was centered near Kansas City. Pressure gradient within it was weak over a large area, and conditions were especially favorable in the northern half of the anticyclone for low temperatures because of the combined effect of radiation and the existence of an already cold air mass. The lowest temperatures of the cold outbreak were recorded on this morning from southern Wisconsin, eastern Iowa, and Missouri, eastward through Ohio.

Figure 16 shows the minimum temperatures reported at selected locations in the northern Plains and North Central States on both the 13th and 14th, also the previous lowest temperature ever recorded at each place. It will be seen that record or near record minima were reported in South Dakota, Nebraska, Kansas, Minnesota, Iowa, Missouri, Wisconsin, Michigan, northern Illinois, Indiana, and Ohio.

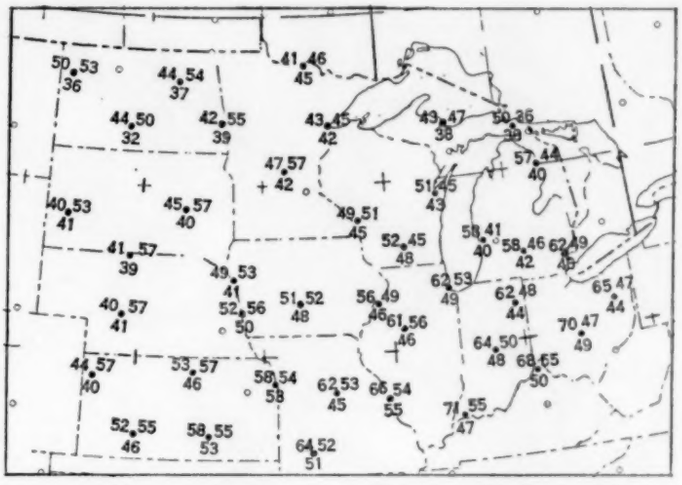


FIGURE 16.—Minimum temperature chart showing the minimum temperature for July 13, 1950 (upper left hand number), minimum temperature for July 14, 1950 (upper right hand number), and the previous record minimum temperature for the month of July (lower number) for selected stations in the northern Plains States and North Central States.

U. S. GOVERNMENT PRINTING OFFICE: 1950

Chart I. Departure (°F.) of the Mean Temperature from the Normal, and Wind Roses for Selected Stations, July 1950

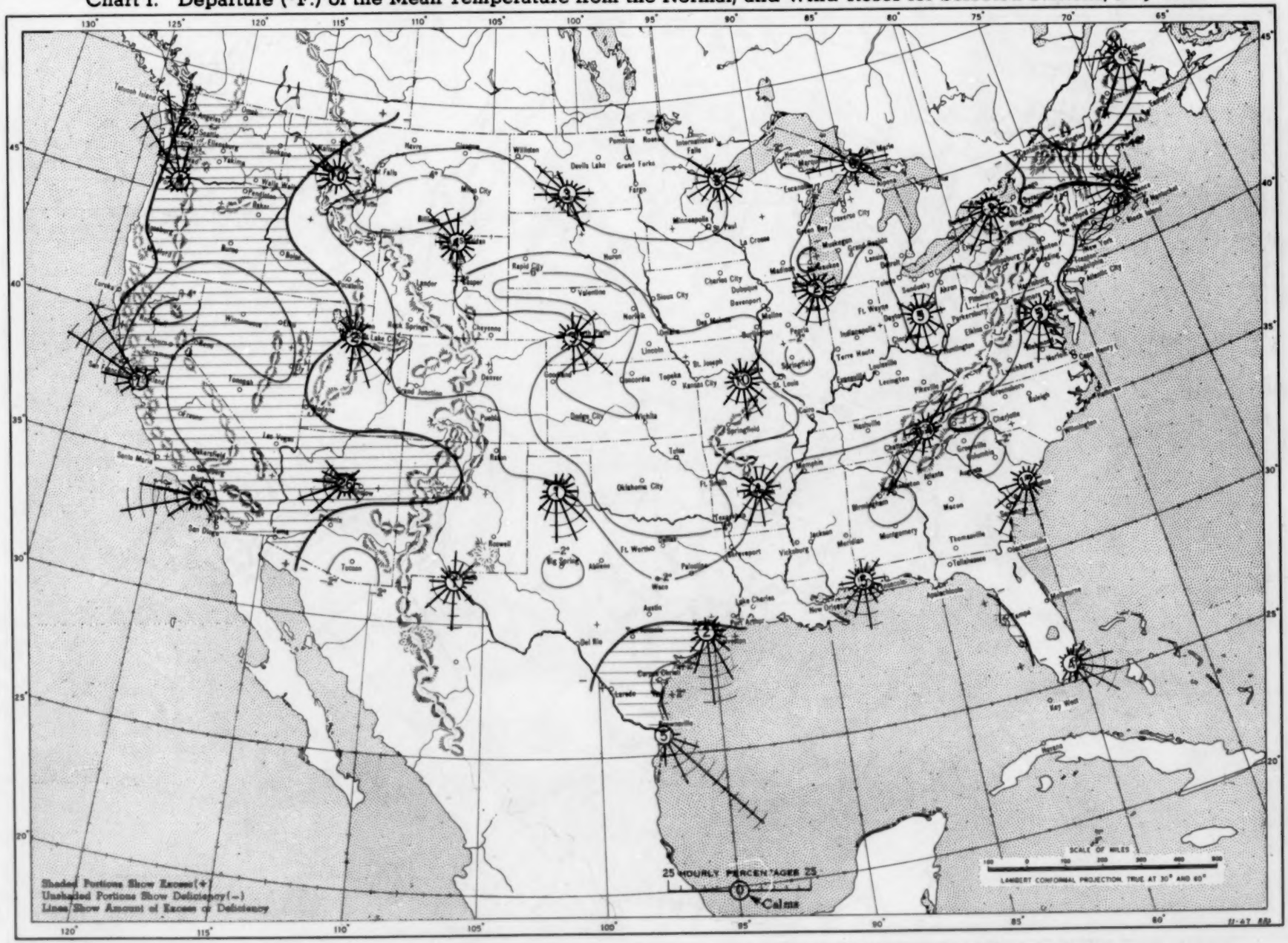

Chart II. Tracks of Centers of Anticyclones, July 1950. (Inset) Departure of Monthly Mean Pressure from Normal

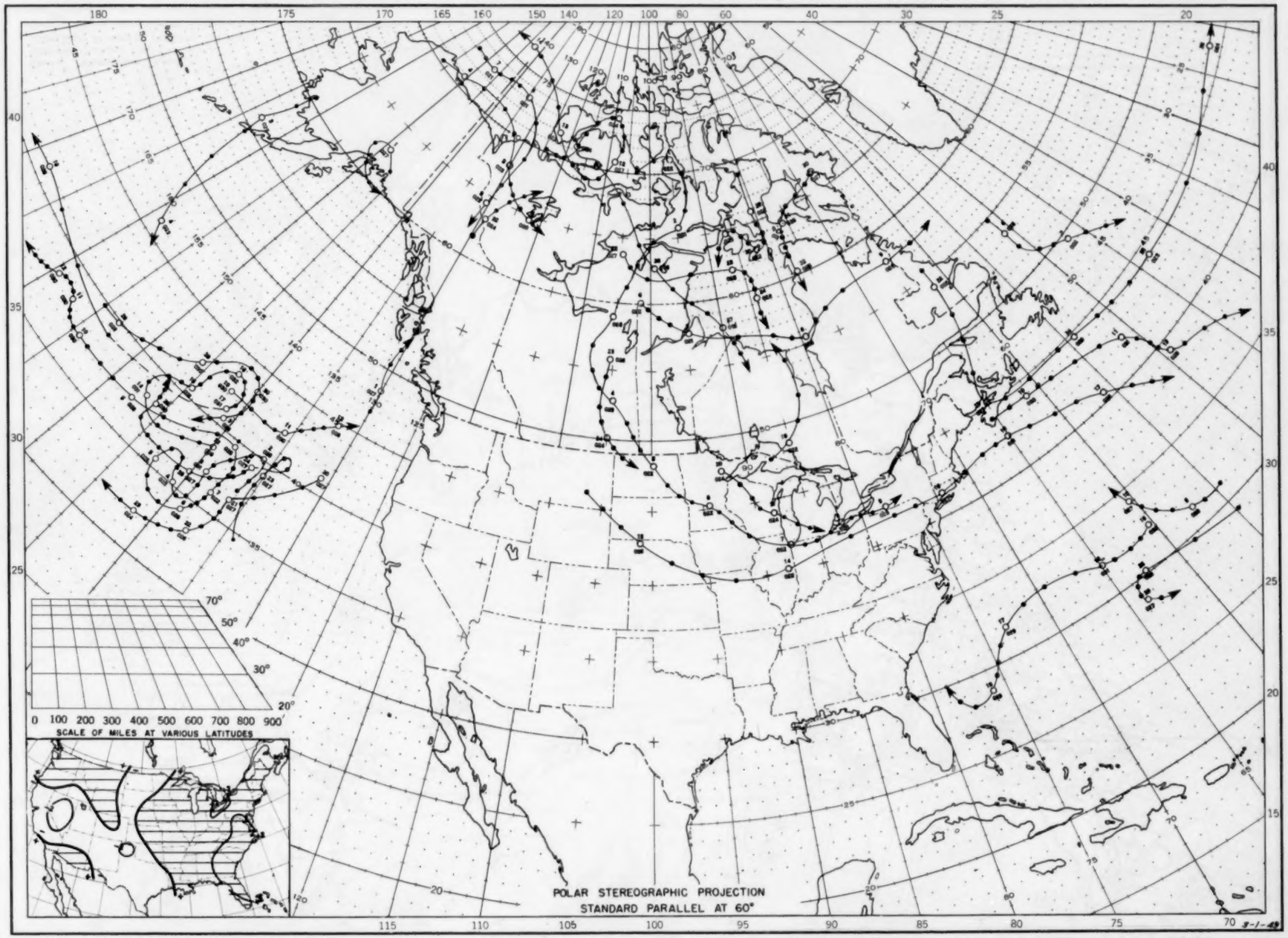


Circle indicates position of anticyclone at 7:30 a. m. (75th meridian time). Dots indicate intervening 6-hourly positions. Figure above circle indicates date, and figure below, pressure to nearest millibar. Only those centers which could be identified for 24 hours or more are included.

**Chart III. Tracks of Centers of Cyclones, July 1950. (Inset) Change in Mean Pressure from Preceding Month**

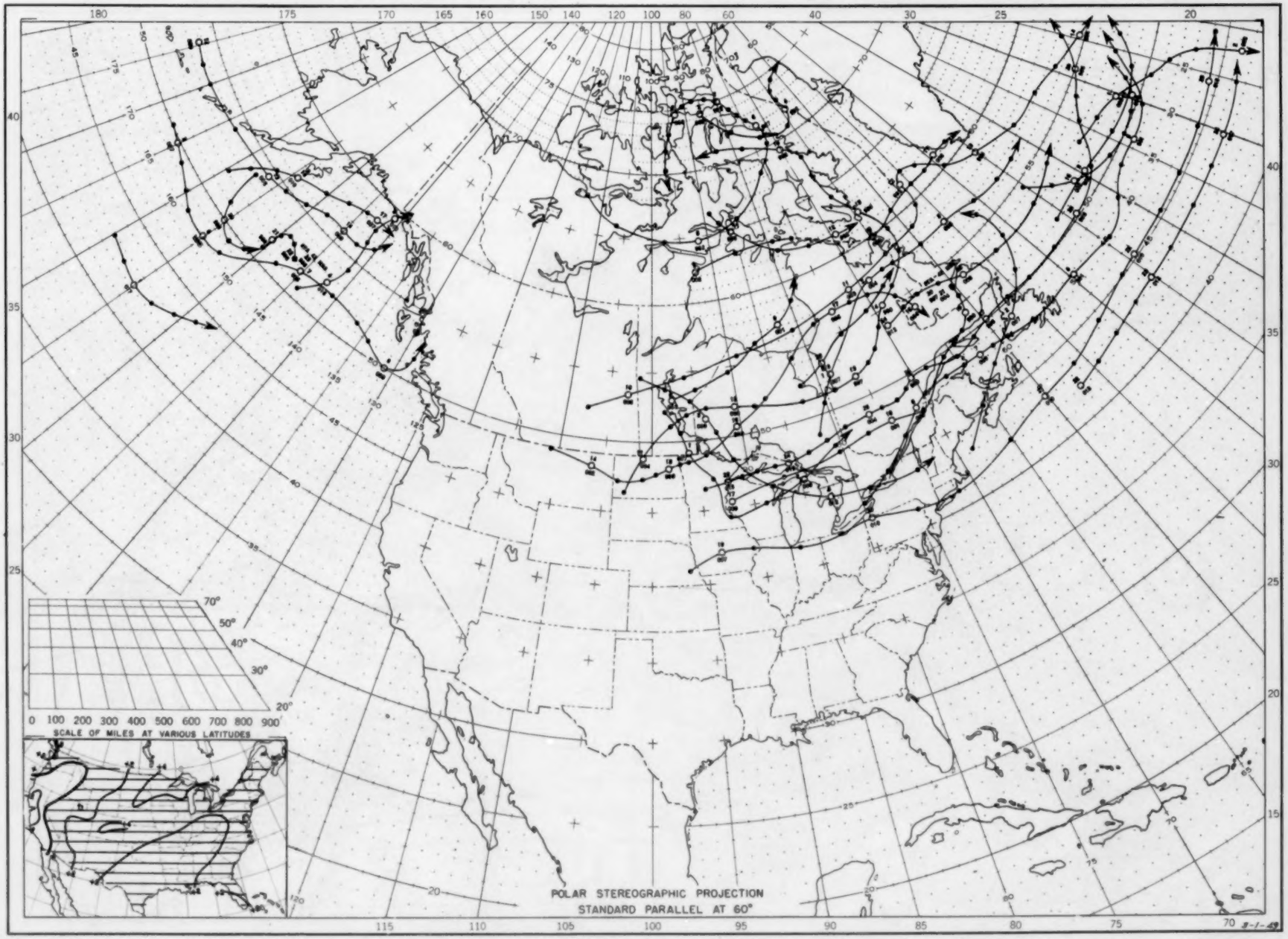


Circle indicates position of cyclone at 7:30 a. m. (75th meridian time) Dots indicate intervening 6-hourly positions. Figure above circle indicates date, and figure below, pressure to nearest millibar. Only those centers which could be identified for 24 hours or more are included.

## Chart IV. Percentage of Clear Sky Between Sunrise and Sunset, July 1950

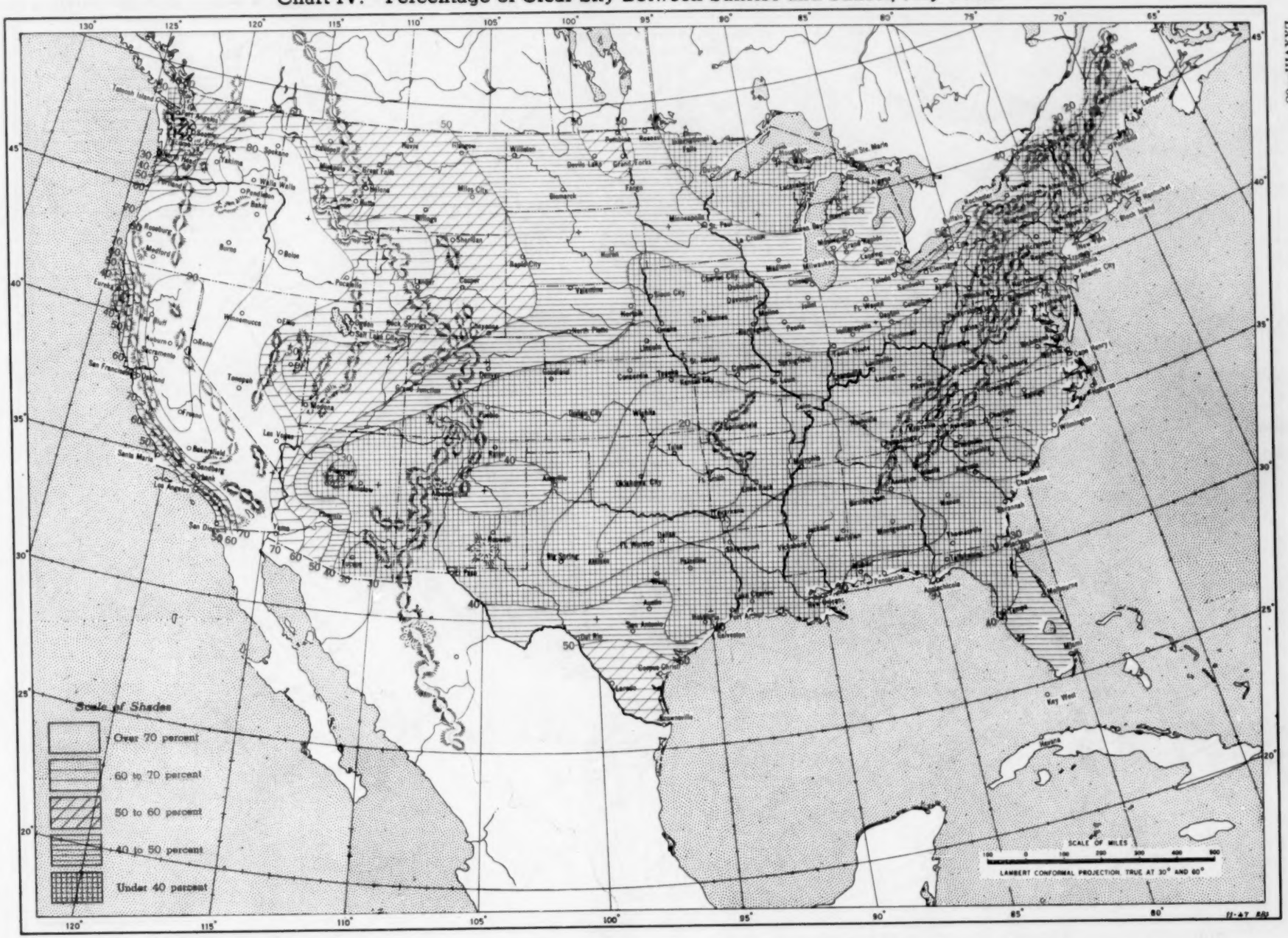

Chart V. Total Precipitation, Inches, July 1950. (Inset) Departure of Precipitation from Normal

Chart VI. Mean Isobars (mb.) at Sea Level and Mean Isotherms (°F.) at Surface, July 1950

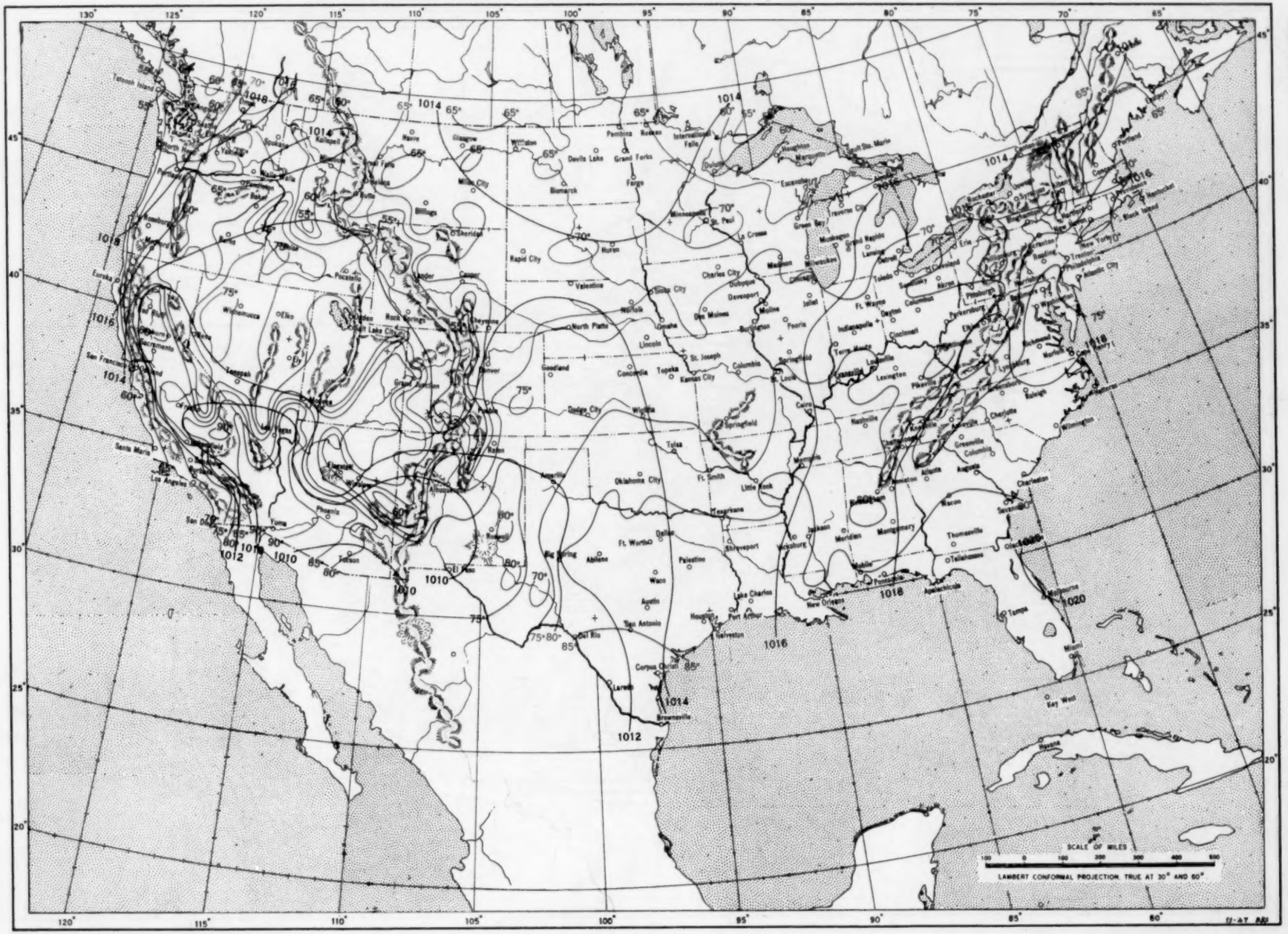

Chart VIII, July 1950. Contour Lines of Mean Dynamic Height (Geopotential) in Units of 0.98 Dynamic Meters and Mean Isotherms in Degrees Centigrade for the 850-millibar Pressure Surface, and Resultant Winds at 1,500 Meters (m. s. l.)

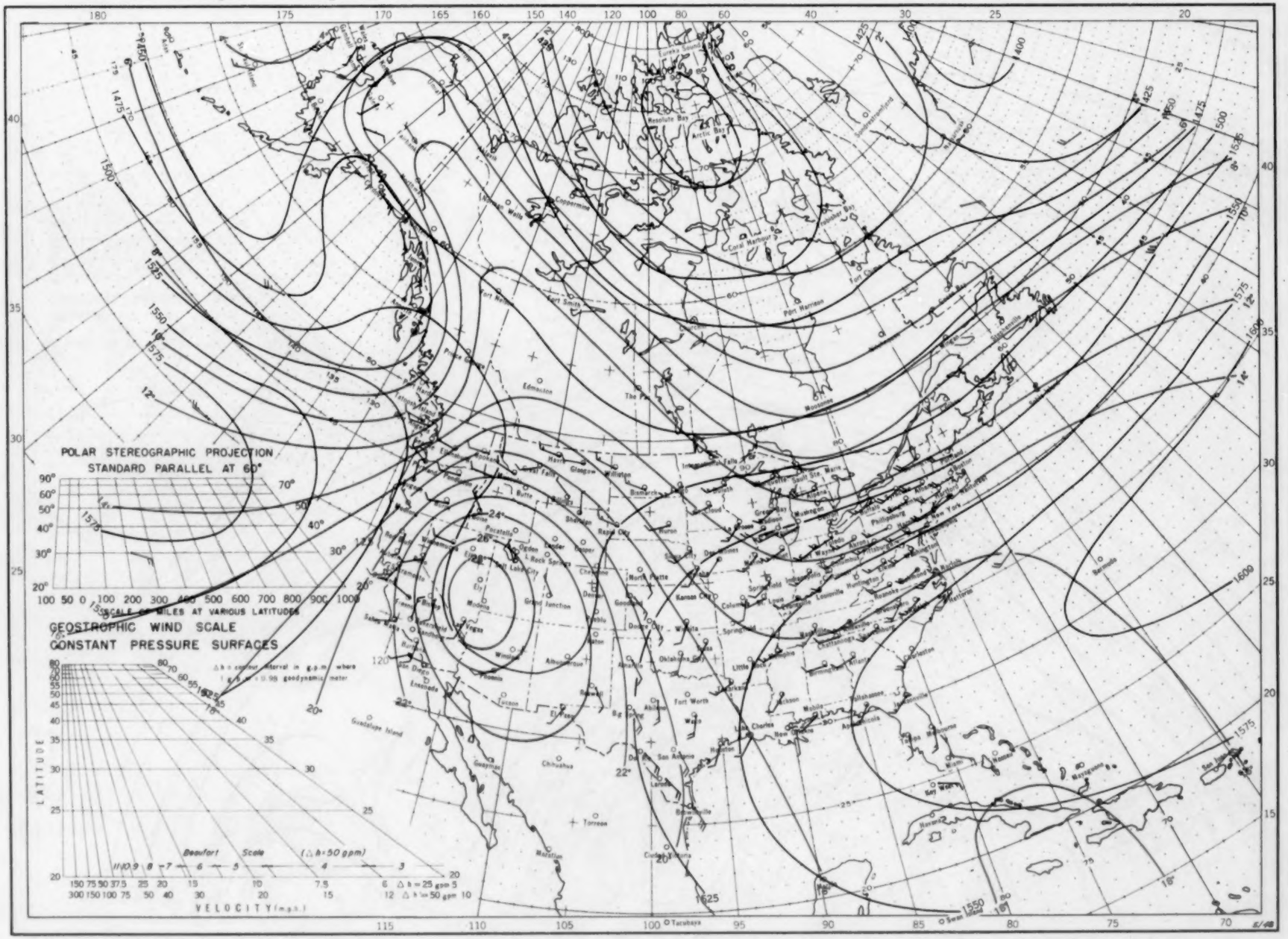


Contour lines and isotherms based on radiosonde observations at 0300 G. C. T. Winds indicated by black arrows based on pilot balloon observations at 2100 G. C. T.; those indicated by red arrows based on rawins taken at 0300 G. C. T.

Chart IX, July 1950. Contour Lines of Mean Dynamic Height (Geopotential) in Units of 0.98 Dynamic Meters and Mean Isotherms in Degrees Centigrade for the 700-millibar Pressure Surface, and Resultant Winds at 3,000 Meters (m. s. l.)

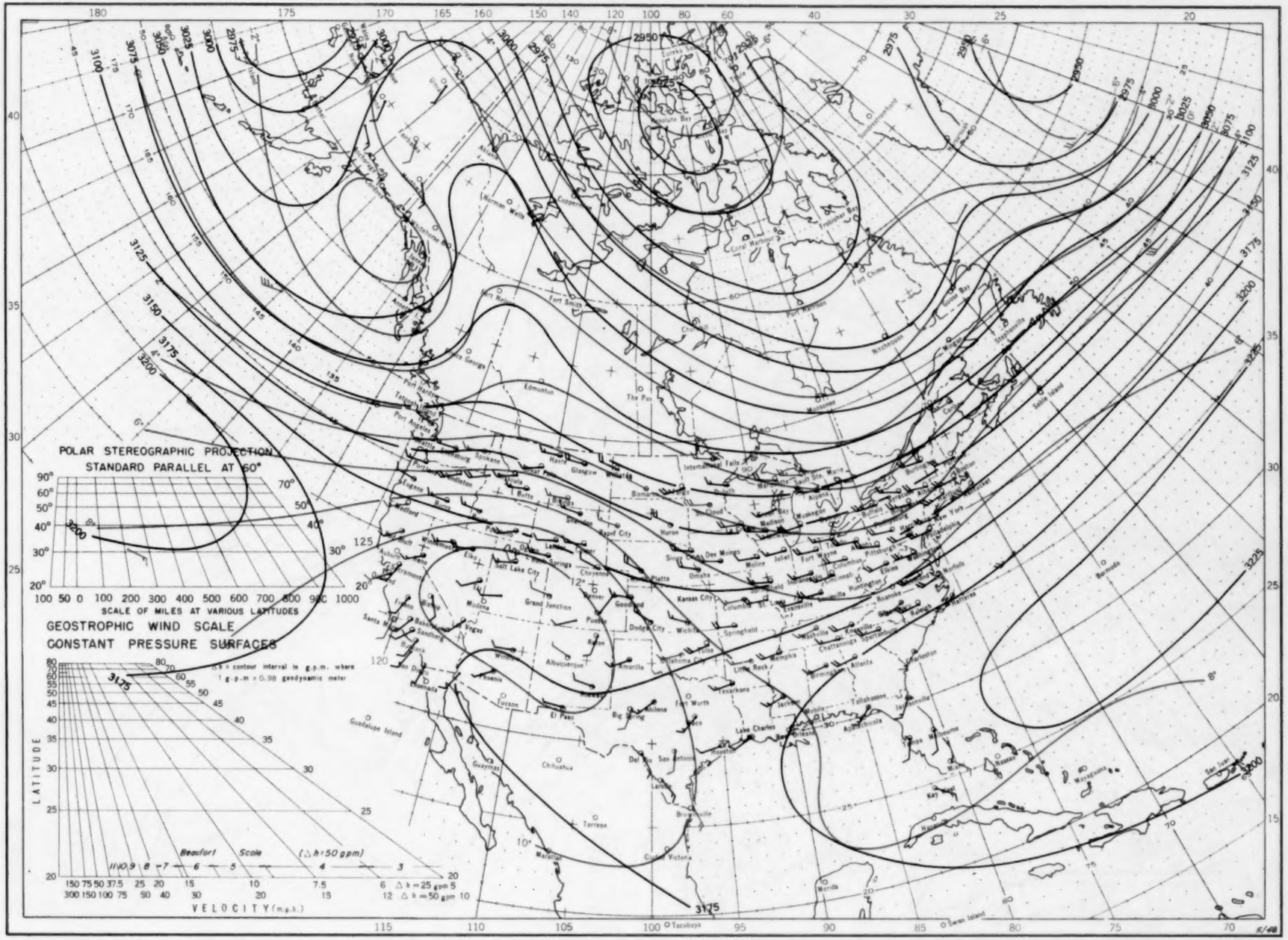


Contour lines and isotherms based on radiosonde observations at 0300 G. C. T. Winds indicated by black arrows based on pilot balloon observations at 2100 G. C. T.; those indicated by red arrows based on rawins taken at 0300 G. C. T.

Chart X, July 1950. Contour Lines of Mean Dynamic Height (Geopotential) in Units of 0.98 Dynamic Meters and Mean Isotherms in Degrees Centigrade for the 500-millibar Pressure Surface, and Resultant Winds at 5,000 Meters (m. s. l.)

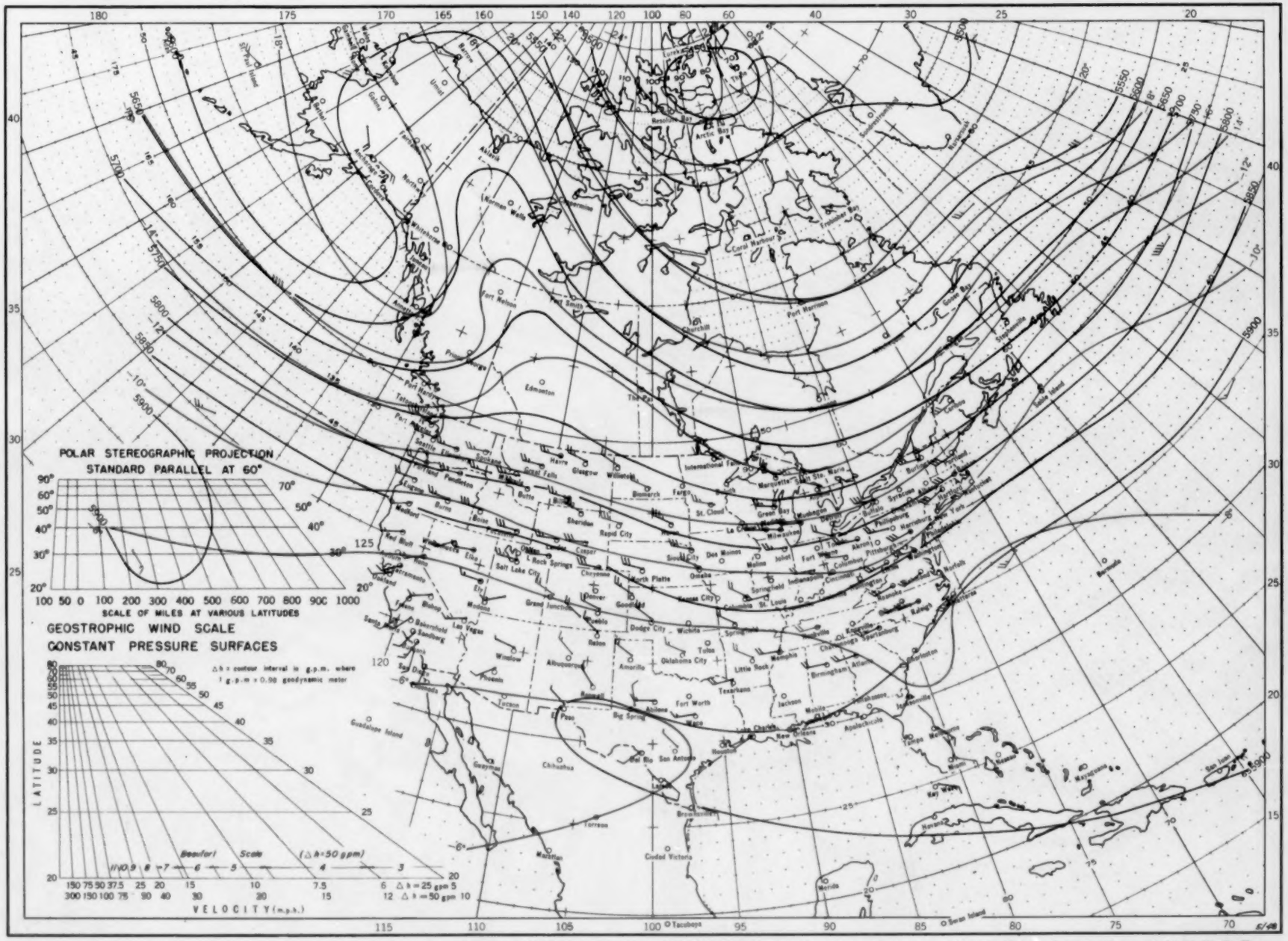


Contour lines and isotherms based on radiosonde observations at 0300 G. C. T. Winds indicated by black arrows based on pilot balloon observations at 2100 G. C. T.; those indicated by red arrows based on rawins taken at 0300 G. C. T.

Chart XI, July 1950. Contour Lines of Mean Dynamic Height (Geopotential) in Units of 0.98 Dynamic Meters and Mean Isotherms in Degrees Centigrade for the 300-millibar Pressure Surface, and Resultant Winds at 10,000 Meters (m. s. l.)

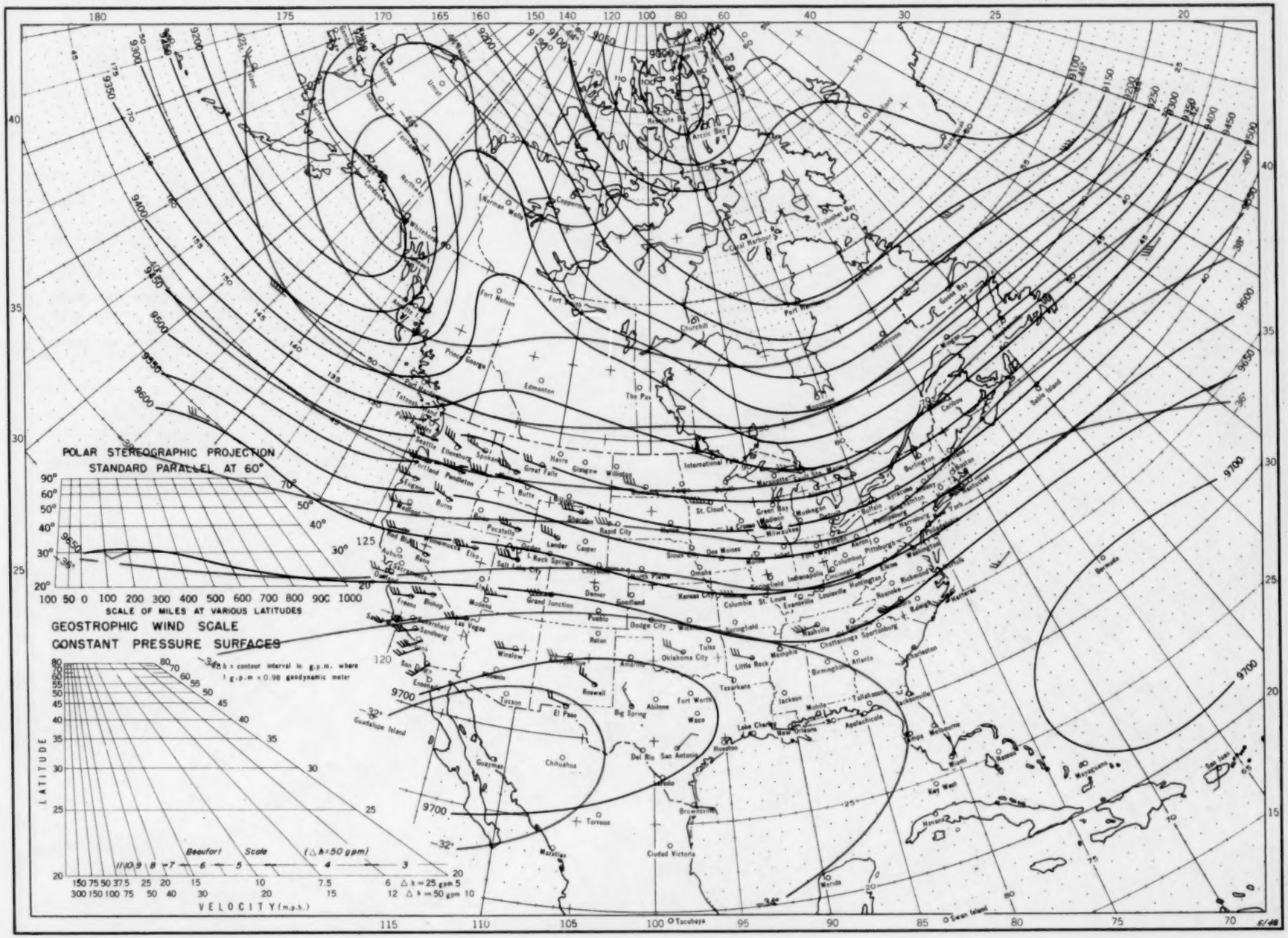


Contour lines and isotherms based on radiosonde observations at 0300 G. C. T. Winds indicated by black arrows based on pilot balloon observations at 2100 G. C. T.; those indicated by red arrows based on rawins taken at 0300 G. C. T.